Regular Article - Experimental Physics

Prompt and non-prompt J/ψ production in pp collisions at $\sqrt{s} = 7$ TeV

The CMS Collaboration[*]

Abstract The production of J/ψ mesons is studied in pp collisions at $\sqrt{s} = 7$ TeV with the CMS experiment at the LHC. The measurement is based on a dimuon sample corresponding to an integrated luminosity of 314 nb^{-1}. The J/ψ differential cross section is determined, as a function of the J/ψ transverse momentum, in three rapidity ranges. A fit to the decay length distribution is used to separate the prompt from the non-prompt (b hadron to J/ψ) component. Integrated over J/ψ transverse momentum from 6.5 to 30 GeV/c and over rapidity in the range $|y| < 2.4$, the measured cross sections, times the dimuon decay branching fraction, are 70.9 ± 2.1(stat.) ± 3.0(syst.) ± 7.8(luminosity) nb for prompt J/ψ mesons assuming unpolarized production and 26.0 ± 1.4(stat.) ± 1.6(syst.) ± 2.9(luminosity) nb for J/ψ mesons from b-hadron decays.

1 Introduction

Heavy-flavour and quarkonium production at hadron colliders provides an important test of the theory of Quantum Chromodynamics (QCD). The production of J/ψ mesons occurs in three ways: prompt J/ψ produced directly in the proton-proton collision, prompt J/ψ produced indirectly (via decay of heavier charmonium states such as χ_c), and non-prompt J/ψ from the decay of a b hadron. This paper presents the first measurement of the differential inclusive, prompt and non-prompt (b hadron) J/ψ production cross sections in pp collisions at a centre-of-mass energy of 7 TeV, in the rapidity range $|y| < 2.4$, by the Compact Muon Solenoid (CMS) experiment.

Despite considerable progress in recent years [1–3], quarkonium production remains puzzling and none of the existing theoretical models satisfactorily describes the prompt J/ψ differential cross section [3–5] and polarization [6] measured at the Tevatron [7]. Measurements at the

Large Hadron Collider (LHC) will contribute to the clarification of the quarkonium production mechanisms by providing differential cross sections in wider rapidity ranges and up to higher transverse momenta than was previously possible, and with corresponding measurements of quarkonium polarization. Cross-section results are largely dependent on the J/ψ polarization, as different polarizations cause different muon momentum spectra in the laboratory frame. Given the sizeable extent of this effect, for prompt J/ψ mesons (where the polarization is presently not well described by the theoretical models) we choose to quote final results for different polarization scenarios, instead of treating this effect as a source of systematic uncertainty.

Non-prompt J/ψ production can be directly related to b-hadron production, leading to a measurement of the b-hadron cross section in pp collisions. Past discrepancies between the Tevatron results (both from inclusive [5] and exclusive [8] measurements) and the next-to-leading-order (NLO) QCD theoretical calculations, were recently resolved using the fixed-order next-to-leading-log (FONLL) approach and updated measurements of the b $\rightarrow$ J/ψ fragmentation and decay [9, 10]. Measured cross-section values and spectra are also found to be in agreement with Monte Carlo generators following this approach, such as MC@NLO [11, 12].

The paper is organized as follows. Section 2 describes the CMS detector. Section 3 presents the data collection, the event trigger and selection, the J/ψ reconstruction, and the Monte Carlo simulation. Section 4 is devoted to the evaluation of the detector acceptance and efficiencies to detect J/ψ events in CMS. In Sect. 5 the measurement of the J/ψ inclusive cross section is reported. In Sect. 6 the fraction of J/ψ events from b-hadron decays is derived, and cross-section results are presented both for prompt J/ψ production and for J/ψ production from b-hadron decays. Section 7 presents comparisons between the measurements and model calculations.

* e-mail: Roberto.Tenchini@cern.ch

2 The CMS detector

The central feature of the CMS apparatus is a superconducting solenoid, of 6 m internal diameter, providing a field of 3.8 T. Within the field volume are the silicon pixel and strip tracker, the crystal electromagnetic calorimeter and the brass/scintillator hadron calorimeter. Muons are detected by three types of gas-ionization detectors embedded in the steel return yoke: Drift Tubes (DT), Cathode Strip Chambers (CSC), and Resistive Plate Chambers (RPC). The measurement covers the pseudorapidity window $|\eta| < 2.4$, where $\eta = -\ln[\tan(\theta/2)]$ and the polar angle θ is measured from the z-axis, which points along the counterclockwise beam direction. The silicon tracker is composed of pixel detectors (three barrel layers and two forward disks on each side of the detector, made of 66 million 100×150 μm^2 pixels) followed by microstrip detectors (ten barrel layers plus three inner disks and nine forward disks on each side of the detector, with 10 million strips of pitch between 80 and 184 μm). Thanks to the strong magnetic field and the high granularity of the silicon tracker, the transverse momentum, p_T, of the muons matched to reconstructed tracks is measured with a resolution of about 1% for the typical muons used in this analysis. The silicon tracker also provides the primary vertex position, with ~ 20 μm accuracy. The first level (L1) of the CMS trigger system, composed of custom hardware processors, uses information from the calorimeters and muon detectors to select the most interesting events. The High Level Trigger (HLT) further decreases the rate before data storage. A much more detailed description of the CMS detector can be found elsewhere [13].

3 Data sample and event reconstruction

3.1 Event selection

The analysis is based on a data sample recorded by the CMS detector in pp collisions at a centre-of-mass energy of 7 TeV. The sample corresponds to a total integrated luminosity of 314 ± 34 nb^{-1}. During this data taking period, there were 1.6 pp collisions per bunch crossing, on average. J/ψ mesons are reconstructed in the $\mu^+\mu^-$ decay channel. The event selection requires good quality data from the tracking, muon, and luminosity detectors, in addition to good trigger conditions.

The analysis is based on events triggered by a double-muon trigger that requires the detection of two independent muon segments at L1, without any further processing at the HLT. All three muon systems, DT, CSC and RPC, take part in the trigger decision. The coincidence of two muon signals, without any cut on p_T, is enough to keep the trigger rate reasonably low at the instantaneous luminosities of the LHC start-up.

Events not coming from pp collisions, such as those from beam-gas interactions or beam-scraping in the transport system near the interaction point, which produce a large activity in the pixel detector, are removed by requiring a good primary vertex to be reconstructed. The primary vertices in the event are found by performing a common fit to tracks for which the points of closest approach to the beam axis are clustered in z, excluding the two muons forming the J/ψ candidate and using adaptive weights to avoid biases from displaced secondary vertices [14]. Given the presence of pile-up, the primary vertex in the event is not unique. According to Monte Carlo simulation studies, the best assignment of the primary vertex is achieved by selecting the one closest in the z coordinate to the dimuon vertex.

3.2 Monte Carlo simulation

Simulated events are used to tune the selection criteria, to check the agreement with data, to compute the acceptance, and to derive corrections to the efficiencies (Sect. 4). Prompt J/ψ mesons have been simulated using Pythia 6.421 [15], which generates events based on the leading-order colour-singlet and colour-octet mechanisms, with non-relativistic QCD (NRQCD) matrix elements tuned by comparing calculations with CDF data [3, 16]. Colour-octet states undergo a shower evolution. Simulated events with b-hadron pairs were also generated with Pythia and the b hadrons decayed inclusively into J/ψ using the EvtGen package [17]. Final-state bremsstrahlung was implemented using PHOTOS [18, 19].

The generated events were passed through the GEANT4-based [20] detector simulation and processed with the same reconstruction program as used for collision events. The detector simulation includes the trigger, as well as the effects of the finite precision of alignment and calibration, as determined using LHC collision data and cosmic-ray muon events [21].

3.3 Offline muon reconstruction

In this analysis, muon candidates are defined as tracks reconstructed in the silicon tracker which are associated with a compatible signal in the muon chambers.

Two different muon reconstruction algorithms are considered. The first one starts from segments in the muon chambers, and provides high-quality and high-purity muon reconstruction for tracks with $p_T \gtrsim 4$ GeV/c in the central pseudorapidity region ($|\eta| \lesssim 1.3$) and $p_T \gtrsim 1$ GeV/c in the forward region; these muons are referred to as *Global Muons*. The second algorithm starts from inner-tracker information, and achieves a better reconstruction efficiency at low momenta; these muons are referred to as *Tracker Muons*. In this case tracks found in the Tracker must be

matched to at least one muon segment in one muon station, the matching being based on angular criteria. There is an overlap between these two reconstruction methods. If a muon is reconstructed by both algorithms, it is assigned to the Global Muon category alone, making the two categories exclusive. Global Muons have a higher reconstruction purity. In both cases, the track momentum is determined by the fit in the silicon tracker.

To reduce muon backgrounds, mostly from decays in flight of kaons and pions, and to ensure good quality reconstructed tracks, muon tracks are required to pass the following requirements: they must have at least 12 hits in the tracker, at least two of which are required to be in the pixel layers, a track fit with a χ^2 per degree of freedom smaller than four, and must pass within a cylinder of radius 3 cm and length 30 cm centred at the primary vertex and parallel to the beam line. If two (or more) tracks are close to each other, it is possible that the same muon segment or set of segments is associated with more than one track. In this case the best track is selected based on the matching between the extrapolated track and the segments in the muon detectors.

The momentum measurement of charged tracks in the CMS detector has systematic uncertainties due to imperfect knowledge of the magnetic field, modelling of the detector material, sub-detector misalignment, and biases in the algorithms which fit the track trajectory; these effects can shift and/or broaden the reconstructed peaks of dimuon resonances. In addition to calibrations already applied to the data [21, 22], residual effects can be determined by studying the dependence of the reconstructed dimuon peak shapes on the muon kinematics. The transverse momentum corrected for the residual scale distortion is parametrized as

$$p_T^{corr} = \left(1 + a_1 + a_2\eta^2\right)p_T^{meas}, \tag{1}$$

where p_T^{meas} is the measured muon transverse momentum. A likelihood fit was performed to the invariant mass shapes to minimize the difference between the reconstructed J/ψ mass and the world-average value [23]. The resulting values of a_1 and a_2 are $(3.8 \pm 1.9) \times 10^{-4}$ and $(3.0 \pm 0.7) \times 10^{-4}$, respectively.

3.4 J/ψ event selection

To select the events with J/ψ decays, muons with opposite charge are paired and their invariant mass is computed. The invariant mass of the muon pair is required to be between 2.6 and 3.5 GeV/c^2. The two muon trajectories are fitted with a common vertex constraint, and events are retained if the fit χ^2 probability is larger than 0.1%. This analysis uses combinations of two Global Muons, two Tracker Muons, and one Global and one Tracker Muon. On average, 1.07 J/ψ
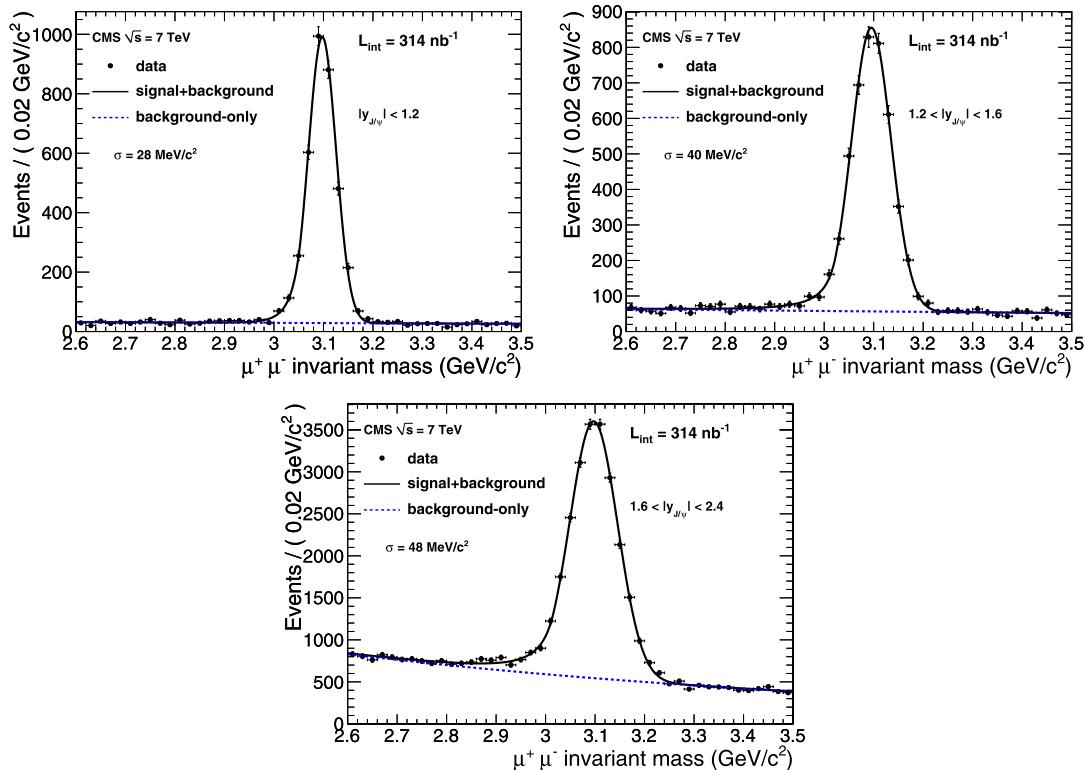

Fig. 1 Opposite-sign dimuon invariant mass distributions in three J/ψ rapidity ranges, fitted with a Crystal Ball function plus an exponential (Sect. 5). The poorer dimuon mass resolution at forward rapidity is caused by the smaller lever arm of the muon tracks

combinations were found per selected dimuon event. In case of multiple combinations in the same event, the one with the purest muon content is chosen. If there are two or more dimuon candidates of the same type (Global-Global, Global-Tracker, or Tracker-Tracker) the one of highest p_T is chosen.

The opposite-sign dimuon mass spectrum is shown in Fig. 1 for three different J/ψ rapidity ranges. About 27 000 J/ψ candidates have been reconstructed, of which about 19% are in the two-Global-Muon category, 54% in the Global-Tracker-Muon category, and the remaining in the two-Tracker-Muon category.

4 Acceptance and efficiency

4.1 Acceptance

The acceptance reflects the finite geometrical coverage of the CMS detector and the limited kinematical reach of the muon trigger and reconstruction systems, constrained by the thickness of the material in front of the muon detectors and by the track curvature in the magnetic field.

The J/ψ acceptance A is defined as the fraction of detectable J/$\psi \to \mu^+\mu^-$ decays, as a function of the dimuon transverse momentum p_T and rapidity y,

$$A(p_T, y; \lambda_\theta) = \frac{N_{\text{det}}(p_T, y; \lambda_\theta)}{N_{\text{gen}}(p_T, y; \lambda_\theta)}, \qquad (2)$$

where N_{det} is the number of detectable J/ψ events in a given (p_T, y) bin, expressed in terms of the dimuon variables after detector smearing, and N_{gen} is the corresponding total number of generated J/ψ events in the Monte Carlo simulation. The parameter λ_θ reflects the fact that the acceptance is computed for various polarization scenarios, as explained below. The large number of simulated events available allows the use of a much smaller bin size for determining A than what is used for the cross-section measurement.

The criteria for detecting the muons coming from the J/ψ decay is that both muons should be within the geometrical acceptance of the muon detectors and have enough

momentum to reach the muon stations. The following kinematic cuts, defining the acceptance region, are chosen so as to guarantee a single-muon detection probability exceeding about 10%:

$p_T^\mu > 3.3$ GeV/c for $|\eta^\mu| < 1.3$;

$p^\mu > 2.9$ GeV/c for $1.3 < |\eta^\mu| < 2.2$;

$p_T^\mu > 0.8$ GeV/c for $2.2 < |\eta^\mu| < 2.4$.

To compute the acceptance, J/ψ events are generated with no cut on p_T and within a rapidity region extending beyond the muon detector's coverage.

The acceptance as a function of p_T and $|y|$ is shown in the left plot of Fig. 2 for the combined prompt and non-prompt J/ψ mesons, with the prompt component decaying isotropically, corresponding to unpolarized production. The right plot of Fig. 2 displays the p_T and $|y|$ distribution of muon pairs measured with an invariant mass within ± 100 MeV/c^2 of the known J/ψ mass [23].

Systematic uncertainties on the acceptance have been investigated, as described in the following paragraphs.

- *Final-state radiation*. At the generator level, the dimuon momentum may differ from the J/ψ momentum, due to final-state radiation (FSR). The difference between the acceptance computed using the dimuon system or the J/ψ variables in (2) is taken as a systematic uncertainty.
- *Kinematical distributions*. Different spectra of the generated J/ψ might produce different acceptances. The difference between using the Pythia spectra and other theoretical calculations (mentioned in Sect. 7) is taken as a systematic uncertainty.
- *b-hadron fraction and polarization*. The J/ψ mesons produced in b-hadron decays can, in principle, have a different acceptance with respect to the prompt ones, due to their different momentum spectra, leading to an uncertainty coming from the unknown proportion of b hadrons in the inclusive sample. The fraction measured in this paper (Sect. 6) has been used to correct the one in the Monte

Fig. 2 *Left*: Acceptance as a function of the J/ψ p_T and rapidity. *Right*: Number of muon pairs within ± 100 MeV/c^2 of the nominal J/ψ mass, in bins of p_T and $|y|$
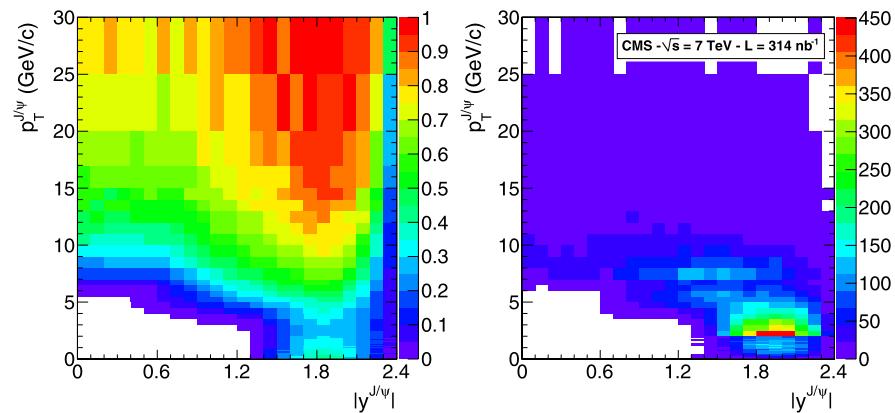
Carlo simulation, and the 20% average accuracy of the measurement has been used to estimate the uncertainty due to this source. For non-prompt J/ψ mesons the b-hadron events are generated with the J/ψ polarization as measured by the BaBar experiment [24], and the corresponding systematic uncertainty is evaluated by taking the difference with respect to the one predicted by EvtGen.

- p_T *calibration and resolution*. A difference between the muon momentum scale in data and simulated events would lead to a different acceptance. The muon transverse momenta have been calibrated as described in Sect. 3.3. The maximum residual bias remaining after the calibration is estimated to be 0.05%. As a conservative estimate, a bias equivalent to this residual uncertainty is applied to the simulated muon momenta. The change in the re-computed acceptance is taken as a systematic uncertainty. Similarly, a difference in the momentum resolution between data and simulated events would also give a different acceptance. The acceptance has been computed with simulated muon momenta smeared according to the resolution measured in data and the difference is taken as a systematic uncertainty.

Finally, the distribution of the z position of the pp interaction point could in principle influence the acceptance. Several Monte Carlo samples of J/ψ mesons have been generated, each coming from different positions along the beam line (between -10 and $+10$ cm with respect to the centre of the collision region) and a negligible variation of the acceptance has been found.

4.2 Efficiency

The single-muon efficiency is computed using the *Tag-and-Probe* method, in a data sample collected with looser trigger requirements. In events with two muon candidates, one candidate, called the "tag", is required to satisfy tight identification criteria. The other candidate, called the "probe", is selected with criteria that depend on the efficiency being measured. The invariant mass of the tag and probe muon candidates must be compatible with the nominal J/ψ mass. Signal yields are obtained for two exclusive subsamples of events, in which the probe muon passes or fails the selection. Fits are performed to the invariant-mass distributions of the "pass" and "fail" subsamples, including terms that account for the background. The efficiency is determined from the relative signal yield in the pass and fail subsamples.

The combined trigger and offline-reconstruction efficiency for a single muon is defined as

$$\epsilon(\mu) = \epsilon_{\text{track}} \cdot \epsilon_{\text{id|track}} \cdot \epsilon_{\text{trig|track+id}}, \tag{3}$$

where ϵ_{track} is the tracking efficiency, $\epsilon_{\text{id|track}}$ is the muon identification efficiency in the muon systems for a tracker-reconstructed muon, and finally $\epsilon_{\text{trig|track+id}}$ is the probability for an offline reconstructed muon to have also fired the trigger.

The tracking efficiency is constant in the momentum range defined by the acceptance cuts, and it varies only slightly in the ϕ–η plane. The muon identification and trigger efficiencies have a stronger p_T^μ and $|\eta^\mu|$ dependence, which is mapped with a finer granularity (nine to twelve p_T^μ and five $|\eta^\mu|$ bins).

The efficiency to detect a given J/ψ event is thus dependent on the value of the muon-pair kinematic variables, and is given by

$$\epsilon(\text{J}/\psi) = \epsilon(\mu^+) \cdot \epsilon(\mu^-) \cdot (1 + \rho) \cdot \epsilon_{\text{vertex}}. \tag{4}$$

The parameter ρ is mainly due to the relatively large bin sizes used to determine the muon efficiencies. While typically $|\rho|$ is smaller than 0.1, in a few bins the values of ρ range from -0.19 and 0.30, corresponding to the regions where the muon efficiencies vary rapidly with respect to the average value, and cannot be effectively determined in the data with the tag-and-probe method, due to the small statistics available. Since the simulation is found to reproduce well the shapes of the muon efficiencies in the data, ρ is evaluated from a large-statistics Monte Carlo sample.

The efficiency for the two muon tracks to be consistent with coming from a common vertex (Sect. 3.4), ϵ_{vertex}, is measured to be $(98.35 \pm 0.16)\%$, by comparing the number of two-Global-Muon combinations within ± 100 MeV/c^2 of the nominal J/ψ mass with and without the common vertex requirement. Given the precision of this estimate, the corresponding systematic uncertainty can be neglected. The following systematic uncertainties on the J/ψ efficiency are considered:

- ρ *parameter*. Any variation of the muon spectrum within each large bin may lead to a different value of ρ. By reweighting the Pythia Monte Carlo simulation, we vary the J/ψ p_T spectrum to reproduce different theoretical predictions (Sect. 7), and take the largest variation as the systematic uncertainty on ρ.

- *Muon efficiency*. The statistical uncertainty on each muon efficiency is propagated using toy Monte Carlo experiments, and the r.m.s. of the newly computed J/ψ efficiencies are assigned as systematic uncertainties. The largest systematic errors are in the bins with less events or in those where the background is largest. When selecting the tag muon, the Tag-and-Probe method produces a slight bias on the kinematics of the probe muon, hence a small difference arises between the measured single-muon efficiencies and those of an unbiased sample. This small effect is studied in the Monte Carlo simulation and corrected for. The whole correction is conservatively taken as a systematic uncertainty on the efficiencies and summed in quadrature with the statistical uncertainty.

5 Inclusive J/ψ cross section

The measurement of the inclusive p_T differential cross section is based on the equation

$$\frac{d^2\sigma}{dp_T\,dy}(J/\psi)\cdot B(J/\psi\rightarrow\mu^+\mu^-)=\frac{N_{corr}(J/\psi)}{\int L\,dt\cdot\Delta p_T\cdot\Delta y}, \quad (5)$$

where $N_{corr}(J/\psi)$ is the J/ψ yield, corrected for the J/ψ acceptance and selection efficiency, in a given transverse momentum-rapidity bin, $\int L\,dt$ is the integrated luminosity, Δp_T and Δy are the sizes of the p_T and rapidity bins, and $B(J/\psi\rightarrow\mu^+\mu^-)$ is the branching ratio of the J/ψ decay into two muons.

5.1 J/ψ yields

The corrected yield, $N_{corr}(J/\psi)$, is determined in two steps. First, in each rapidity and p_T bin an unbinned maximum likelihood fit to the $\mu^+\mu^-$ invariant mass distribution is performed. The resulting yield is then corrected by a factor that takes into account the average acceptance (A) and detection efficiency (ϵ) in the bin under consideration.

In the mass fits, the shape assumed for the signal is a Crystal Ball function [25], which takes into account

the detector resolution as well as the radiative tail from bremsstrahlung. The shape of the underlying continuum is described by an exponential. Table 1 lists the J/ψ uncorrected signal yields and the corresponding statistical uncertainties from the fit, for the chosen bins.

Different functions were used to assess systematic effects coming from the fit function chosen to model the signal and the continuum shapes. For the signal, the Crystal Ball function was varied to a sum of a Crystal Ball and a Gaussian, while for the background a second-order polynomial was used. The maximum difference in the result was taken as a systematic uncertainty. The uncertainty is particularly large for the low-p_T bins, where the signal purity is the smallest.

Additionally, a bias on the muon momentum scale can shift the events from one J/ψ p_T bin to the adjacent ones. To estimate this systematic effect, a bias has been applied to the muon momenta equal to the residual uncertainty on the scale after the calibration, as explained in Sect. 3.4, and a negligible variation was found.

5.2 Inclusive J/ψ cross section results

The previously discussed systematic uncertainties affecting the inclusive J/ψ cross section are listed in Table 2. In addition, the relative error on the luminosity determination

Table 1 Uncorrected event yield (with its statistical error from the fit) in each p_T bin, together with the average acceptance times efficiency with (computed in the unpolarized production scenario); the uncertainty on the acceptance times efficiency is the sum of the statistical and systematic errors

$p_T^{J/\psi}$ (GeV/c)	Yield	$\langle 1/(A\epsilon)\rangle^{-1}$	$p_T^{J/\psi}$ (GeV/c)	Yield	$\langle 1/(A\epsilon)\rangle^{-1}$
$|y| < 1.2$			$1.6 < |y| < 2.4$		
6.5–8.0	726.5 ± 28.3	0.084 ± 0.005	0.00–0.50	695.6 ± 40.7	0.075 ± 0.008
8.0–10.0	868.1 ± 30.7	0.178 ± 0.005	0.50–0.75	829.3 ± 44.7	0.079 ± 0.010
10.0–12.0	513.2 ± 23.5	0.288 ± 0.008	0.75–1.00	1006.0 ± 48.8	0.078 ± 0.010
12.0–30.0	636.0 ± 26.1	0.405 ± 0.008	1.00–1.25	1216.8 ± 52.8	0.079 ± 0.010
$1.2 < |y| < 1.6$			1.25–1.50	1232.9 ± 53.7	0.077 ± 0.008
2.0–3.5	414.9 ± 38.0	0.016 ± 0.001	1.50–1.75	1252.9 ± 50.3	0.075 ± 0.008
3.5–4.5	401.7 ± 23.2	0.035 ± 0.004	1.75–2.00	1132.7 ± 57.5	0.074 ± 0.006
4.5–5.5	618.9 ± 28.9	0.086 ± 0.004	2.00–2.25	1122.7 ± 55.0	0.071 ± 0.006
5.5–6.5	690.9 ± 34.0	0.167 ± 0.005	2.25–2.50	899.9 ± 39.4	0.074 ± 0.006
6.5–8.0	712.0 ± 28.0	0.247 ± 0.006	2.50–2.75	903.3 ± 72.4	0.075 ± 0.004
8.0–10.0	463.7 ± 23.3	0.334 ± 0.009	2.75–3.00	757.6 ± 36.2	0.077 ± 0.005
10.0–30.0	406.2 ± 22.4	0.445 ± 0.010	3.00–3.25	756.1 ± 35.7	0.082 ± 0.005
			3.25–3.50	703.6 ± 33.6	0.084 ± 0.004
			3.50–4.00	1150.2 ± 40.0	0.092 ± 0.005
			4.00–4.50	991.8 ± 35.8	0.100 ± 0.004
			4.50–5.50	1441.4 ± 42.6	0.117 ± 0.005
			5.50–6.50	993.0 ± 34.7	0.157 ± 0.008
			6.50–8.00	900.6 ± 35.1	0.193 ± 0.008
			8.00–10.00	604.3 ± 26.8	0.250 ± 0.007
			10.00–30.00	462.6 ± 23.6	0.309 ± 0.010

Table 2 Relative systematic uncertainties on the corrected yield for different J/ψ rapidity bins. The variation range over the different p_T bins is given. In general, uncertainties depend only weakly on the p_T values, except for the fit function systematic uncertainty, which de- creases with increasing p_T due to the better purity of the signal. The large excursion of the muon efficiency systematic uncertainty reflects changes in the event yield and in the signal purity among the p_T bins

| Affected quantity	Source	Relative error (%)		
		$|y| < 1.2$	$1.2 < |y| < 1.6$	$1.6 < |y| < 2.4$
Acceptance	FSR	0.8–2.5	0.3–1.6	0.0–0.9
	p_T calibration and resolution	1.0–2.5	0.8–1.2	0.1–1.0
	Kinematical distributions	0.3–0.8	0.6–2.6	0.9–3.1
	b-hadron fraction and polarization	1.9–3.1	0.5–1.2	0.2–3.0
Efficiency	Muon efficiency	1.9–5.1	2.3–12.2	2.7–9.2
	ρ parameter	0.5–0.9	0.6–8.1	0.2–7.1
Yields	Fit function	0.6–1.1	0.4–5.3	0.3–8.8
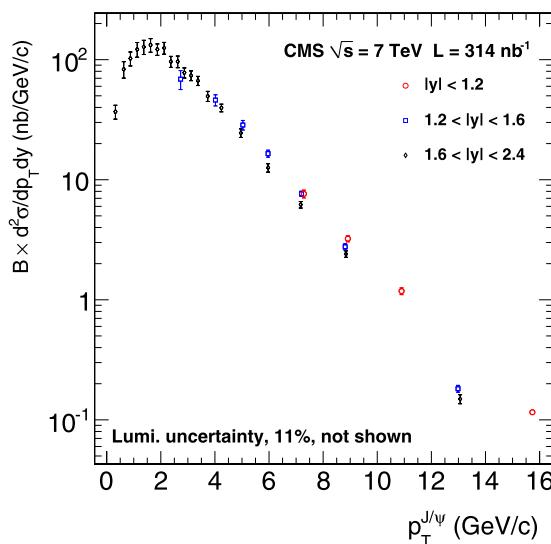
Fig. 3 Differential inclusive J/ψ cross section as a function of p_T for the three different rapidity intervals and in the unpolarized production scenario. The errors on the ordinate values are the statistical and systematic errors added in quadrature. The 11% uncertainty due to the luminosity determination is not shown and is common to all bins

is 11%, and is common to all bins. Table 3 reports the values of the resulting J/ψ differential cross section, for different polarization scenarios: unpolarized, full longitudinal polarization and full transverse polarization in the Collins-Soper or the helicity frames [7]. The average p_T in Table 3 has been computed as the mean p_T of the events in an invariant mass region of ± 100 MeV/c^2 around the J/ψ peak value, after subtracting the background contribution, estimated by the sidebands.

Figure 3 shows the inclusive differential cross section $\frac{d^2\sigma}{dp_T\,dy} \cdot \mathrm{B}(\mathrm{J}/\psi \to \mu^+\mu^-)$ in the three rapidity ranges, showing statistical and systematic uncertainties, except the luminosity uncertainty, added in quadrature. It should be noted that the first bin in the forward rapidity region extends down to zero J/ψ p_T.

The total cross section for inclusive J/ψ production, obtained by integrating over p_T between 6.5 and 30 GeV/c and over rapidity between -2.4 and 2.4, in the unpolarized production hypothesis, gives

$$\sigma(pp \to \mathrm{J}/\psi + X) \cdot \mathrm{B}(\mathrm{J}/\psi \to \mu^+\mu^-)$$
$$= 97.5 \pm 1.5(\text{stat.}) \pm 3.4(\text{syst.}) \pm 10.7(\text{luminosity}) \text{ nb.} \tag{6}$$

6 Fraction of J/ψ from b-hadron decays

The measurement of the fraction of J/ψ yield coming from b-hadron decays relies on the discrimination of the J/ψ mesons produced away from the pp collision vertex, determined by the distance between the dimuon vertex and the primary vertex in the plane orthogonal to the beam line.

The primary vertex is determined as described in Sect. 3.1, but excluding the two muons from the J/ψ decays. Given the presence of pile-up, the primary vertex in the event is not unique. According to Monte Carlo simulation studies, the best assignment of the primary vertex is achieved by selecting the one closest in the z coordinate to the dimuon vertex.

6.1 Separating prompt and non-prompt J/ψ

As an estimate of the b-hadron proper decay length, the quantity $\ell_{\mathrm{J}/\psi} = L_{xy} \cdot m_{\mathrm{J}/\psi}/p_T$ is computed for each J/ψ candidate, where $m_{\mathrm{J}/\psi}$ is the J/ψ mass [23] and L_{xy} is the most probable transverse decay length in the laboratory frame [26, 27]. L_{xy} is defined as

$$L_{xy} = \frac{\mathbf{u}^T \sigma^{-1} \mathbf{x}}{\mathbf{u}^T \sigma^{-1} \mathbf{u}}, \tag{7}$$

Table 3 Differential inclusive cross sections and average p_T in the bin (see text), for each prompt J/ψ polarization scenario considered: unpolarized ($\lambda_\theta = 0$), full longitudinal polarization ($\lambda_\theta = -1$) and full transverse polarization ($\lambda_\theta = +1$) in the Collins–Soper (CS) or the helicity (HX) frames [7]. For the unpolarized case, the first error is statistical and the second is systematic; for the others the total error is given

$p_T^{J/\psi}$ (GeV/c)	$\langle p_T^{J/\psi}\rangle$ (GeV/c)	$\frac{d^2\sigma}{dp_T\,dy} \cdot B(J/\psi \to \mu^+\mu^-)$ (nb/GeV/c)				
		$\lambda_\theta = 0$	$\lambda_\theta^{CS} = -1$	$\lambda_\theta^{CS} = +1$	$\lambda_\theta^{HX} = -1$	$\lambda_\theta^{HX} = +1$
$\|y\| < 1.2$						
6.50–8.00	7.29	$7.63 \pm 0.30 \pm 0.97$	9.28 ± 1.20	6.99 ± 0.91	5.70 ± 0.74	9.14 ± 1.20
8.00–10.00	8.91	$3.23 \pm 0.11 \pm 0.38$	3.81 ± 0.47	3.00 ± 0.37	2.45 ± 0.30	3.85 ± 0.48
10.00–12.00	10.90	$1.18 \pm 0.05 \pm 0.14$	1.35 ± 0.17	1.10 ± 0.14	0.93 ± 0.12	1.37 ± 0.17
12.00–30.00	15.73	$0.116 \pm 0.005 \pm 0.013$	0.130 ± 0.016	0.110 ± 0.013	0.096 ± 0.012	0.129 ± 0.016
$1.2 < \|y\| < 1.6$						
2.00–3.50	2.73	$68.8 \pm 6.3 \pm 13.0$	50.4 ± 9.9	84.6 ± 19.0	50.5 ± 9.9	84.5 ± 19.0
3.50–4.50	4.02	$46.1 \pm 2.7 \pm 6.5$	37.3 ± 5.7	52.8 ± 8.4	33.9 ± 5.2	56.4 ± 8.8
4.50–5.50	5.03	$28.6 \pm 1.3 \pm 3.9$	28.2 ± 4.1	28.7 ± 4.1	20.8 ± 3.0	35.0 ± 5.0
5.50–6.50	5.96	$16.5 \pm 0.8 \pm 2.0$	17.8 ± 2.3	16.0 ± 2.0	12.3 ± 1.6	20.1 ± 2.6
6.50–8.00	7.20	$7.64 \pm 0.30 \pm 0.87$	8.71 ± 1.10	7.19 ± 0.87	5.80 ± 0.71	9.19 ± 1.10
8.00–10.00	8.81	$2.76 \pm 0.14 \pm 0.32$	3.11 ± 0.39	2.62 ± 0.33	2.18 ± 0.27	3.24 ± 0.41
10.00–30.00	12.99	$0.182 \pm 0.010 \pm 0.021$	0.204 ± 0.026	0.173 ± 0.022	0.151 ± 0.019	0.202 ± 0.026
$1.6 < \|y\| < 2.4$						
0.00–0.50	0.32	$36.8 \pm 2.2 \pm 6.0$	26.1 ± 4.5	46.5 ± 8.0	26.3 ± 4.5	45.6 ± 7.8
0.50–0.75	0.63	$83.2 \pm 4.5 \pm 15.3$	59.5 ± 11.3	105.1 ± 19.9	60.4 ± 11.6	103.2 ± 19.3
0.75–1.00	0.88	$102.3 \pm 5.0 \pm 16.9$	72.8 ± 13.3	128.9 ± 23.7	75.1 ± 13.4	125.0 ± 22.8
1.00–1.25	1.13	$121.9 \pm 5.3 \pm 21.1$	87.1 ± 14.8	152.4 ± 27.1	91.11 ± 18.2	146.2 ± 25.6
1.25–1.50	1.37	$127.7 \pm 5.6 \pm 21.6$	91.1 ± 15.6	160.1 ± 29.3	96.2 ± 17.7	152.9 ± 28.4
1.50–1.75	1.62	$132.5 \pm 5.3 \pm 21.9$	94.7 ± 15.8	165.9 ± 27.7	101.3 ± 16	157.8 ± 25.4
1.75–2.00	1.87	$121.9 \pm 6.2 \pm 17.9$	87.4 ± 13.6	152.1 ± 24.7	93.6 ± 14.9	143.9 ± 23.1
2.00–2.25	2.12	$125.2 \pm 6.1 \pm 18.7$	89.8 ± 13.9	156.3 ± 24.7	97.1 ± 14.9	147.3 ± 23.6
2.25–2.50	2.37	$96.3 \pm 4.2 \pm 14.1$	69.0 ± 10.2	120.5 ± 18.1	74.3 ± 11	114 ± 16.8
2.50–2.75	2.63	$96.4 \pm 7.7 \pm 13.0$	69.8 ± 11.1	119.3 ± 18.6	74.8 ± 11.8	113.2 ± 18.1
2.75–3.00	2.87	$77.9 \pm 3.7 \pm 10.7$	56.3 ± 8.0	96.4 ± 13.9	60.3 ± 8.5	91.6 ± 13.1
3.00–3.25	3.12	$73.7 \pm 3.5 \pm 10.0$	53.8 ± 7.7	91.2 ± 13.0	57.6 ± 8.3	86.5 ± 13.0
3.25–3.50	3.37	$66.7 \pm 3.2 \pm 8.8$	48.5 ± 6.9	82.8 ± 12.0	52.1 ± 7.3	78.3 ± 11.0
3.50–4.00	3.74	$49.6 \pm 1.7 \pm 7.1$	37.0 ± 5.5	60.6 ± 9.0	39.0 ± 5.8	58.3 ± 8.6
4.00–4.50	4.24	$39.7 \pm 1.4 \pm 5.0$	30.0 ± 4.0	47.3 ± 6.3	31.4 ± 4.2	46.0 ± 6.1
4.50–5.50	4.96	$24.5 \pm 0.7 \pm 3.3$	19.3 ± 2.6	28.7 ± 4.0	19.6 ± 2.7	28.2 ± 3.9
5.50–6.50	5.97	$12.6 \pm 0.4 \pm 1.7$	10.8 ± 1.4	14.0 ± 1.9	10.3 ± 1.4	14.3 ± 1.9
6.50–8.00	7.17	$6.20 \pm 0.24 \pm 0.74$	5.70 ± 0.72	6.61 ± 0.84	5.13 ± 0.65	6.94 ± 0.88
8.00–10.00	8.84	$2.41 \pm 0.11 \pm 0.28$	2.41 ± 0.31	2.44 ± 0.31	2.04 ± 0.26	2.64 ± 0.34
10.00–30.00	13.06	$0.149 \pm 0.008 \pm 0.019$	0.155 ± 0.021	0.148 ± 0.021	0.132 ± 0.019	0.161 ± 0.023

where **x** is the vector joining the vertex of the two muons and the primary vertex of the event, in the transverse plane, **u** is the unit vector of the J/ψ p_T, and σ is the sum of the primary and secondary vertex covariance matrices.

To determine the fraction f_B of J/ψ mesons from b-hadron decays in the data, we perform an unbinned maximum-likelihood fit in each p_T and rapidity bin. The dimuon mass spectrum and the $\ell_{J/\psi}$ distribution are simultaneously fit by a log-likelihood function,

$$\ln L = \sum_{i=1}^{N} \ln F(\ell_{J/\psi}, m_{\mu\mu}), \qquad (8)$$

where N is the total number of events and $m_{\mu\mu}$ is the invariant mass of the muon pair. The expression for $F(\ell_{J/\psi}, m_{\mu\mu})$ is

$$F(\ell_{J/\psi}, m_{\mu\mu}) = f_{Sig} \cdot F_{Sig}(\ell_{J/\psi}) \cdot M_{Sig}(m_{\mu\mu})$$
$$+ (1 - f_{Sig}) \cdot F_{Bkg}(\ell_{J/\psi}) \cdot M_{Bkg}(m_{\mu\mu}) \quad (9)$$

where:

- f_{Sig} is the fraction of events attributed to J/ψ sources coming from both prompt and non-prompt components;
- $M_{Sig}(m_{\mu\mu})$ and $M_{Bkg}(m_{\mu\mu})$ are functional forms describing the invariant dimuon mass distributions for the signal and background, respectively, as detailed in Sect. 5.1;
- $F_{Sig}(\ell_{J/\psi})$ and $F_{Bkg}(\ell_{J/\psi})$ are functional forms describing the $\ell_{J/\psi}$ distribution for the signal and background, respectively.

The signal part is given by a sum of prompt and non-prompt components,

$$F_{Sig}(\ell_{J/\psi}) = f_B \cdot F_B(\ell_{J/\psi}) + (1 - f_B) \cdot F_p(\ell_{J/\psi}), \quad (10)$$

where f_B is the fraction of J/ψ from b-hadron decays, and $F_p(\ell_{J/\psi})$ and $F_B(\ell_{J/\psi})$ are the $\ell_{J/\psi}$ distributions for prompt and non-prompt J/ψ, respectively.

As $\ell_{J/\psi}$ should be zero in an ideal detector for prompt events, $F_p(\ell_{J/\psi})$ is described simply by a resolution function. The core of the resolution function is taken to be a double-Gaussian and its parameters are allowed to float in the nominal fit. Since $\ell_{J/\psi}$ depends on the position of the primary vertex, an additional Gaussian component is added, to take into account possible wrong assignments of the primary vertex; its parameters are fixed from the Monte Carlo simulation.

The $\ell_{J/\psi}$ shape of the non-prompt component in (10) is given by convolving the same resolution function with the true $\ell_{J/\psi}$ distribution of the J/ψ from long-lived b hadrons, as given by the Monte Carlo simulation.

For the background $\ell_{J/\psi}$ distribution $F_{Bkg}(\ell_{J/\psi})$, the functional form employed by CDF [5] is used:

$$F_{Bkg}(x) = (1 - f_+ - f_- - f_{sym}) R(x)$$
$$+ \left[\frac{f_+}{\lambda_+} e^{-\frac{x'}{\lambda_+}} \theta(x') + \frac{f_-}{\lambda_-} e^{\frac{x'}{\lambda_-}} \theta(-x') \right.$$
$$\left. + \frac{f_{sym}}{2\lambda_{sym}} e^{-\frac{|x'|}{\lambda_{sym}}} \right] \otimes R(x' - x), \qquad (11)$$

where $R(x)$ is the resolution model mentioned above, f_i ($i = \{+, -, sym\}$) are the fractions of the three long-lived components with mean decay lengths λ_i, and $\theta(x)$ is the step function. The fractions f_i are left free in the fit, while the effective parameters λ_i are previously determined with a fit to the $\ell_{J/\psi}$ distribution in the sidebands of the dimuon invariant mass distribution, defined as the regions 2.6–2.9 and 3.3–3.5 GeV/c^2.

The parameter f_B (b fraction) is determined in the same rapidity regions as used to present the inclusive production cross section but some p_T bins are grouped, since more events per bin are needed to determine all fit parameters. Figure 4 shows the projection of the likelihood fits in two sample bins. The full results are reported in Table 4, where f_B has been corrected by the prompt/non-prompt acceptances, as discussed in Sect. 4. The fitting procedure has been tested in five sample bins using toy experiments, which establish reasonable goodness-of-fit and exclude the possibility of biases in the f_B determination.

Figure 5 shows the measured b fraction. It increases strongly with p_T. At low p_T, essentially all J/ψ mesons are promptly produced, whereas at $p_T \sim 12$ GeV/c around one third come from beauty decays. This pattern does not show a significant change with rapidity (within the current uncertainties) over the window covered by the CMS detector. The CMS results are compared to the higher-precision data of CDF [5], obtained in proton-antiproton collisions at $\sqrt{s} = 1.96$ TeV. It is interesting to note that the increase with p_T of the b fraction is very similar between the two experiments, the CMS points being only slightly higher, despite the different collision energies.

6.1.1 Systematic uncertainties affecting the b-fraction result

Several sources of systematic uncertainty have been addressed and are described in the following lines.

- *Residual misalignments in the tracker.* The effect of uncertainties in the measured misalignment of the tracker modules is estimated by reconstructing the data several times using different sets of alignment constants. These sets reflect the uncertainty in the constants and, in particular, explore possible deformations of the tracker which are poorly constrained by the data [21]. The largest difference between the results with the nominal set of constants and with these sets is taken as a systematic uncertainty.

Fig. 4 Projection in the $\ell_{J/\psi}$ dimension of the two-dimensional likelihood fit (in mass and $\ell_{J/\psi}$) in the bins $2 < p_T < 4.5$ GeV/c, $1.2 < |y| < 1.6$ (*left*) and $6.5 < p_T < 10$ GeV/c, $1.6 < |y| < 2.4$ (*right*), with their pull distributions (*bottom*)
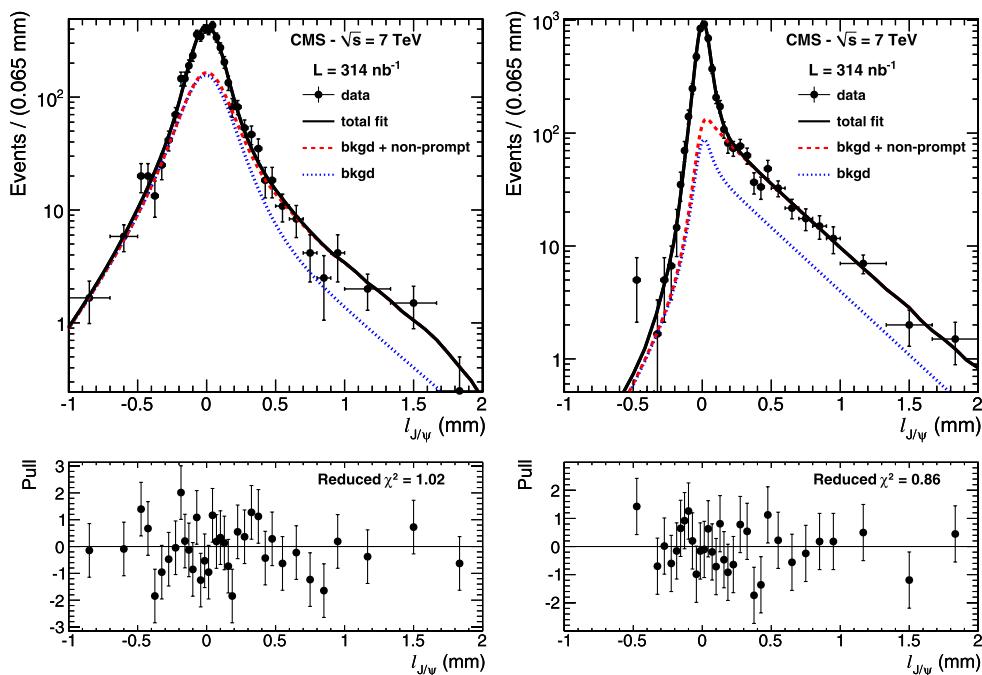
Table 4 Fit results for the determination of the fraction of J/ψ mesons from b hadrons in p_T and $|y|$ bins, corrected by the prompt and non-prompt acceptances. The average p_T per bin is also quoted. The two uncertainties in the b-fraction values are statistical and systematic, respectively

$|y|$	p_T (GeV/c)	$\langle p_T \rangle$ (GeV/c)	b fraction
0–1.2	6.5–10.0	8.14	$0.257 \pm 0.015 \pm 0.014$
	10.0–30.0	13.50	$0.395 \pm 0.018 \pm 0.005$
1.2–1.6	2.0–4.5	3.27	$0.146 \pm 0.021 \pm 0.028$
	4.5–6.5	5.48	$0.180 \pm 0.017 \pm 0.019$
	6.5–10.0	7.89	$0.203 \pm 0.017 \pm 0.014$
	10.0–30.0	12.96	$0.360 \pm 0.031 \pm 0.016$
1.6–2.4	0.00 − 1.25	0.79	$0.057 \pm 0.021 \pm 0.042$
	1.25–2.00	1.60	$0.087 \pm 0.014 \pm 0.022$
	2.00–2.75	2.35	$0.113 \pm 0.013 \pm 0.020$
	2.75–3.50	3.10	$0.139 \pm 0.014 \pm 0.010$
	3.50–4.50	3.96	$0.160 \pm 0.014 \pm 0.013$
	4.50–6.50	5.35	$0.177 \pm 0.012 \pm 0.012$
	6.50–10.00	7.86	$0.235 \pm 0.016 \pm 0.012$
	10.00–30.00	13.11	$0.374 \pm 0.031 \pm 0.008$
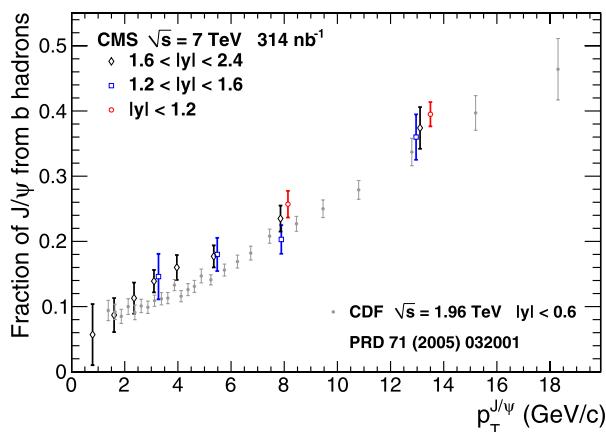
Fig. 5 Fraction of the J/ψ production cross section originating from b-hadron decays, as a function of the J/ψ p_T, as measured by CMS in three rapidity bins and by CDF, at a lower collision energy

- *b-hadron lifetime model.* In an alternative approach, $\ell_{J/\psi}$ is described by a convolution of an exponential decay with a Gaussian function, which describes the smearing due to the relative motion of the J/ψ with respect to the parent b hadron. The difference between the nominal Monte Carlo template model and this alternative is taken as a systematic uncertainty.
- *Primary vertex estimation.* In an alternative approach, the beam spot as calculated on a run-by-run basis is chosen as the primary vertex in calculating $\ell_{J/\psi}$, and the fit is repeated. The difference is taken as a systematic uncertainty.
- *Background.* The background is fitted using only the sidebands and the result is used as input to the fit in the signal region. The effect of a ± 100 MeV/c^2 variation in the sideband boundaries is taken as a systematic uncertainty.

- $\ell_{\mathrm{J}/\psi}$ *resolution model*. The nominal (triple-Gaussian) fit model for the decay length resolution is compared to a model using two Gaussians only, fixing the "additional" Gaussian to be zero. The difference is taken as a systematic uncertainty.
- *Different prompt and non-prompt efficiencies*. The Monte Carlo simulation predicts small differences between the prompt and non-prompt J/ψ efficiencies. These are taken into account and the relative difference assumed as a systematic uncertainty.

A summary of all systematic effects and their importance is given in Table 5.

Table 5 Summary of relative systematic uncertainties in the b-fraction yield (in %). The variation range over the different p_T bins is given in the three rapidity regions. In general, uncertainties are p_T-dependent and decrease with increasing p_T

	$|y| < 1.2$	$1.2 < |y| < 1.6$	$1.6 < |y| < 2.4$
Tracker misalignment	0.5–0.7	0.9–4.6	0.7–9.1
b-lifetime model	0.0–0.1	0.5–4.8	0.5–11.2
Vertex estimation	0.3	1.0–12.3	0.9–65.8
Background fit	0.1–4.7	0.5–9.5	0.2–14.8
Resolution model	0.8–2.8	1.3–13.0	0.4–30.2
Efficiency	0.1–1.1	0.3–1.3	0.2–2.4

6.1.2 Prompt and non-prompt J/ψ production cross sections

The prompt J/ψ cross section and the cross section from b-hadron decays, together with their statistical and systematic uncertainties, are given in Tables 6 and 7, respectively, for the different polarization scenarios considered in Sect. 5.

The total cross section for prompt J/ψ production times B(J/$\psi \to \mu^+\mu^-$), for the unpolarized production scenario, has been obtained by integrating the differential cross section over p_T between 6.5 and 30 GeV/c and over rapidity between -2.4 and 2.4,

$$\mathrm{B}\big(\mathrm{J}/\psi \to \mu^+\mu^-\big) \cdot \sigma(\mathrm{pp} \to \text{prompt J}/\psi)$$
$$= 70.9 \pm 2.1 \pm 3.0 \pm 7.8 \text{ nb}, \tag{12}$$

where the three uncertainties are statistical, systematic and due to the measurement of the integrated luminosity, respectively. Similarly, the cross section of non-prompt J/ψ mesons from b-hadron decays, times B(J/$\psi \to \mu^+\mu^-$), is

$$\mathrm{B}\big(\mathrm{J}/\psi \to \mu^+\mu^-\big) \cdot \sigma(\mathrm{pp} \to bX \to \mathrm{J}/\psi\,X)$$
$$= 26.0 \pm 1.4 \pm 1.6 \pm 2.9 \text{ nb}. \tag{13}$$

The sum of these two cross sections differs slightly from the inclusive value, which was determined assuming a b fraction taken from Monte Carlo expectations.

Table 6 Differential prompt J/ψ cross sections for each polarization scenario considered: unpolarized ($\lambda_\theta = 0$), full longitudinal polarization ($\lambda_\theta = -1$) and full transverse polarization ($\lambda_\theta = +1$) in the Collins–Soper (CS) or the Helicity (HX) frames [7]. For the unpolarized case, the first error is statistical and the second is systematic; for the others the total error is given

p_T (GeV/c)	$\mathrm{B}(\mathrm{J}/\psi \to \mu^+\mu^-) \cdot \frac{d^2\sigma_{\mathrm{prompt}}}{dp_\mathrm{T}\,dy}$ (nb/GeV/c) $\lambda_\theta = 0$	$\lambda_\theta^{\mathrm{CS}} = -1$	$\lambda_\theta^{\mathrm{CS}} = +1$	$\lambda_\theta^{\mathrm{HX}} = -1$	$\lambda_\theta^{\mathrm{HX}} = +1$
$|y| < 1.2$					
6.5–10.0	$3.76 \pm 0.13 \pm 0.47$	4.63 ± 0.60	3.45 ± 0.45	2.63 ± 0.34	4.79 ± 0.62
10.0–30.0	$0.134 \pm 0.033 \pm 0.016$	0.161 ± 0.044	0.123 ± 0.033	0.099 ± 0.026	0.164 ± 0.045
$1.2 < |y| < 1.6$					
2.0–4.5	$50.6 \pm 3.6 \pm 8.4$	36.4 ± 6.5	63.6 ± 11.6	36.3 ± 6.5	63.1 ± 11.4
4.5–6.5	$18.4 \pm 0.7 \pm 2.4$	17.3 ± 2.3	19.1 ± 2.6	13.3 ± 1.8	22.7 ± 3.1
6.5–10.0	$3.85 \pm 0.15 \pm 0.44$	4.11 ± 0.49	3.74 ± 0.45	2.87 ± 0.34	4.67 ± 0.56
10.0–30.0	$0.116 \pm 0.009 \pm 0.014$	0.127 ± 0.018	0.111 ± 0.015	0.093 ± 0.013	0.133 ± 0.019
$1.6 < |y| < 2.4$					
0.00–1.25	$71.9 \pm 2.4 \pm 11.2$	49.7 ± 7.9	92.5 ± 14.7	51.0 ± 8.1	90.3 ± 14.3
1.25–2.00	$116.2 \pm 3.5 \pm 16.8$	80.8 ± 11.9	149.1 ± 22.0	86.7 ± 12.8	140.7 ± 20.8
2.00–2.75	$93.7 \pm 3.4 \pm 12.4$	65.8 ± 9.1	118.8 ± 16.3	72.7 ± 10.0	110.3 ± 15.2
2.75–3.50	$62.6 \pm 2.0 \pm 7.9$	44.5 ± 5.7	78.8 ± 10.2	49.1 ± 6.4	72.7 ± 9.5
3.50–4.50	$37.4 \pm 1.1 \pm 4.9$	27.4 ± 3.7	45.7 ± 6.2	29.9 ± 4.1	42.8 ± 5.8
4.50–6.50	$15.2 \pm 0.4 \pm 2.0$	11.9 ± 1.6	18.0 ± 2.4	12.6 ± 1.7	17.1 ± 2.3
6.50–10.00	$3.08 \pm 0.11 \pm 0.37$	2.79 ± 0.35	3.36 ± 0.42	2.64 ± 0.33	3.37 ± 0.42
10.00–30.00	$0.093 \pm 0.007 \pm 0.012$	0.092 ± 0.014	0.096 ± 0.014	0.082 ± 0.012	0.100 ± 0.015

Table 7 Differential non-prompt J/ψ cross section times the J/ψ branching ratio to dimuons, assuming the polarization measured by the BaBar experiment [24] at the $\Upsilon(4S)$. The first uncertainty is statistical and the second is systematic

$p_T^{J/\psi}$ (GeV/c)	$B(J/\psi \to \mu^+\mu^-) \cdot \frac{d^2\sigma_{\text{non-prompt}}}{dp_T \, dy}$ (nb/GeV/c)
$\|y\| < 1.2$	
6.5–10.0	$1.30 \pm 0.08 \pm 0.19$
10.0–30.0	$0.087 \pm 0.024 \pm 0.010$
$1.2 < \|y\| < 1.6$	
2.0–4.5	$8.67 \pm 1.36 \pm 2.71$
4.5–6.5	$4.04 \pm 0.41 \pm 0.79$
6.5–10.0	$0.98 \pm 0.09 \pm 0.11$
10.0–30.0	$0.065 \pm 0.007 \pm 0.008$
$1.6 < \|y\| < 2.4$	
0.00–1.25	$4.31 \pm 1.59 \pm 3.54$
1.25–2.00	$11.0 \pm 1.8 \pm 4.2$
2.00–2.75	$11.9 \pm 1.4 \pm 3.4$
2.75–3.50	$10.1 \pm 1.1 \pm 1.6$
3.50–4.50	$7.19 \pm 0.65 \pm 1.25$
4.50–6.50	$3.28 \pm 0.24 \pm 0.53$
6.50–10.00	$0.95 \pm 0.07 \pm 0.13$
10.00–30.00	$0.055 \pm 0.005 \pm 0.007$
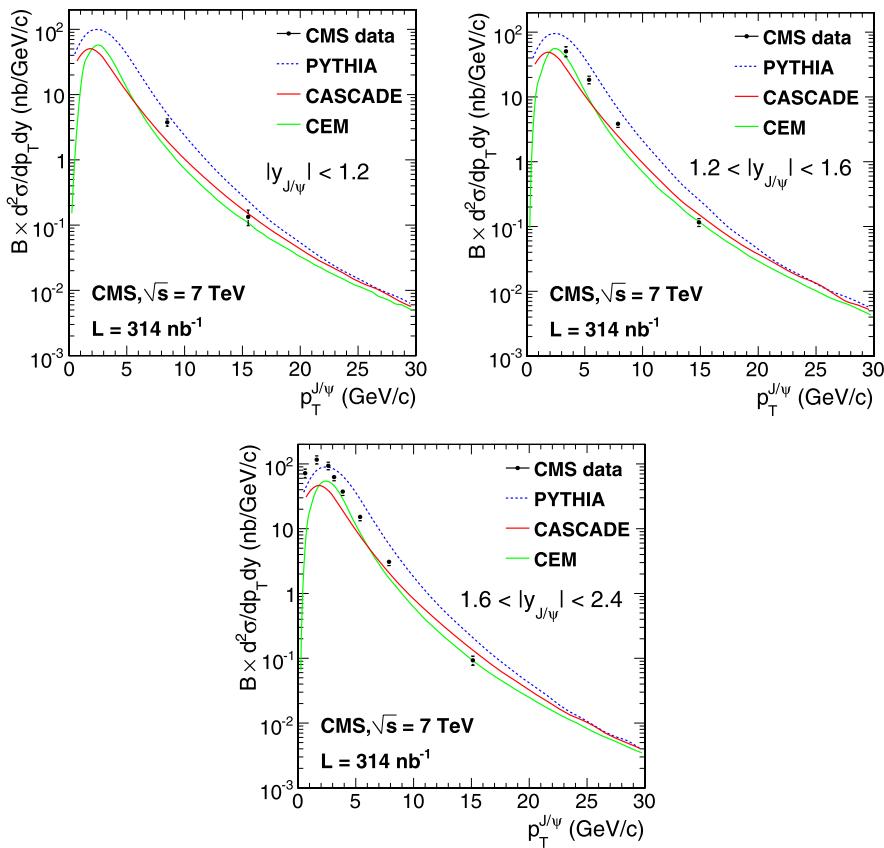
7 Comparison with theoretical calculations

The prompt J/ψ differential production cross sections, in the rapidity ranges considered in the analysis, as summarized in Table 6, were compared with calculations made with the Pythia [15] event generator (see also Sect. 3.2), the CASCADE [28, 29] event generator (including colour-singlet contributions, and based on k_T factorization and CCFM unintegrated gluon PDFs), as well as with the Colour Evaporation Model (CEM) [30–34]. These calculations include the contributions to the prompt J/ψ yield due to feed-down decays from heavier charmonium states (χ_c and $\psi(2S)$) and can, therefore, be directly compared to the measured data points, as shown in Fig. 6.

In contrast, it is not possible to compare our measurement with the predictions of models such as the Colour-Singlet Model (including higher-order corrections) [35–38] or the LO NRQCD framework (which includes singlet and octet components) [39, 40] , because they are only available for the direct J/ψ production component, while the measurements include a significant contribution from feed-down decays, of the order of 30% [41, 42]. Very recently, predictions including the feed-down contribution have become available at NLO in the NRQCD framework [43]. At forward rapidity and low p_T the calculations shown in Fig. 6 underestimate the measured yield.

Fig. 6 Differential prompt J/ψ production cross section, as a function of p_T for the three different rapidity intervals. The data points are compared with three different models, using the PYTHIA curve to calculate the abscissa where they are plotted [44]

Fig. 7 Differential non-prompt J/ψ production cross section, as a function of p_T for the three different rapidity intervals. The data points are compared with three different models, using the PYTHIA curve to calculate the abscissa where they are plotted [44]
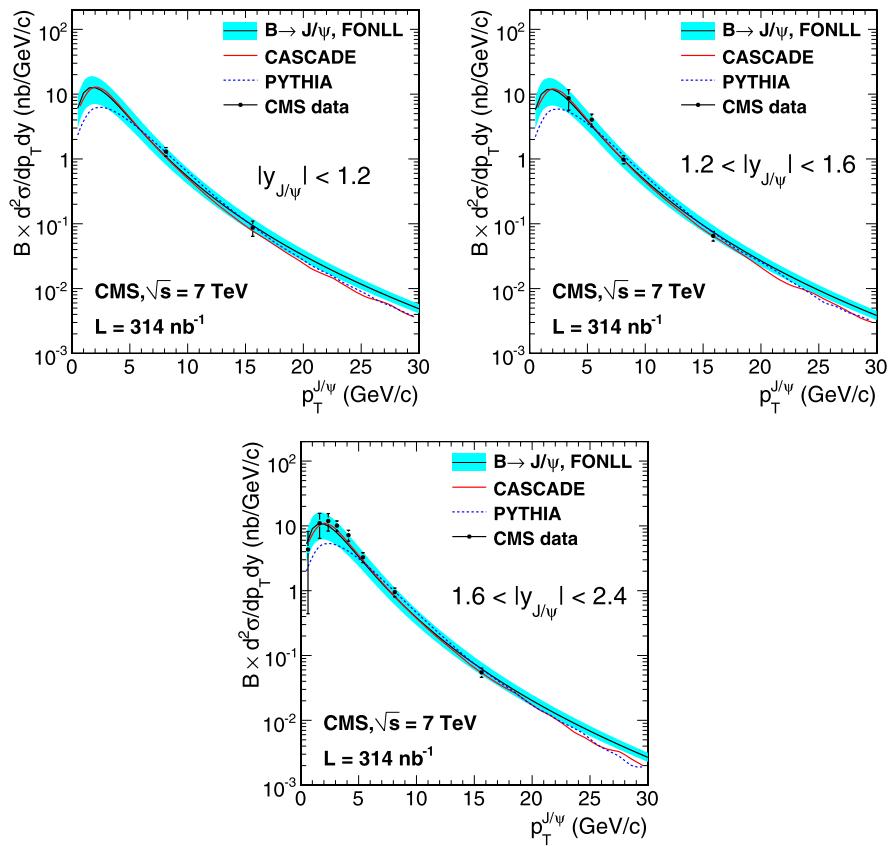
The non-prompt J/ψ differential production cross sections, as summarized in Table 7, have been compared with calculations made with the Pythia and CASCADE Monte Carlo generators, and in the FONLL framework [10]. The measured results are presented in Fig. 7. The agreement with FONLL and CASCADE is excellent, while Pythia tends to underestimate the yield below 5 GeV/c in p_T.

8 Conclusions

We have presented the first measurement of the J/ψ production cross section in pp collisions at $\sqrt{s} = 7$ TeV, based on 314 nb^{-1} of integrated luminosity collected by the CMS experiment during the first months of LHC operation.

The p_T differential J/ψ production cross section, in the dimuon decay channel, has been measured in three rapidity ranges, starting at zero p_T for $1.6 < |y| < 2.4$, at 2 GeV/c for $1.2 < |y| < 1.6$, and at 6.5 GeV/c for $|y| < 1.2$. The measured total cross section for prompt J/ψ production in the unpolarized scenario, in the dimuon decay channel, is

$$\sigma(pp \to J/\psi + X) \cdot B\big(J/\psi \to \mu^+\mu^-\big)$$

$$= 70.9 \pm 2.1(\text{stat.}) \pm 3.0(\text{syst.}) \pm 7.8(\text{luminosity}) \text{ nb},$$

for transverse momenta between 6.5 and 30 GeV/c and in the rapidity range $|y| < 2.4$. Aside from the luminosity con-

tribution, the systematic uncertainty is dominated by the statistical precision of the muon efficiency determination from data.

The measured total cross section times $B(J/\psi \to \mu^+\mu^-)$ for J/ψ production due to b-hadron decays, for $6.5 < p_T < 30$ GeV/c and $|y| < 2.4$, is

$$\sigma(pp \to bX \to J/\psi X) \cdot B\big(J/\psi \to \mu^+\mu^-\big)$$

$$= 26.0 \pm 1.4(\text{stat.}) \pm 1.6(\text{syst.}) \pm 2.9(\text{luminosity}) \text{ nb.}$$

The differential prompt and non-prompt measurements have been compared with theoretical calculations. A reasonable agreement is found between data and theory for the non-prompt case while the measured prompt J/ψ cross section exceeds the expectations at forward rapidity and low p_T.

References

1. N. Brambilla et al., CERN Yellow Report, CERN-2005-005 (2005)
2. J.P. Lansberg, J/ψ, ψ' and Υ production at hadron colliders: a review. Int. J. Mod. Phys. A **21**, 3857 (2006). doi:10.1142/S0217751X06033180
3. M. Krämer, Quarkonium production at high-energy colliders. Prog. Part. Nucl. Phys. **47**, 141 (2001). doi:10.1016/S0146-6410(01)00154-5
4. CDF Collaboration, J/ψ and $\psi(2S)$ production in $p\bar{p}$ collisions at $\sqrt{s} = 1.8$ TeV. Phys. Rev. Lett. **79**, 572 (1997). doi:10.1103/PhysRevLett.79.572
5. CDF Collaboration, Measurement of the J/ψ meson and b-hadron production cross section in $p\overline{p}$ collisions at $\sqrt{s} = 1960$ GeV. Phys. Rev. D **71**, 032001 (2005). doi:10.1103/PhysRevD.71.032001
6. CDF Collaboration, Polarization of J/ψ and $\psi(2S)$ mesons produced in $p\bar{p}$ collisions at $\sqrt{s} = 1.96$ TeV. Phys. Rev. Lett. **99**, 132001 (2007). doi:10.1103/PhysRevLett.99.132001
7. P. Faccioli et al., Towards the experimental clarification of quarkonium polarization. Eur. Phys. J. C **69**, 657 (2010). doi:10.1140/epjc/s10052-010-1420-5
8. CDF Collaboration, Measurement of the B^+ production cross-section in $p\bar{p}$ collisions at $\sqrt{s} = 1.96$ TeV. Phys. Rev. D **75**, 012010 (2007). doi:10.1103/PhysRevD.75.012010
9. M. Cacciari, M. Greco, P. Nason, The p_T spectrum in heavy-flavour hadroproduction. J. High Energy Phys. **9805**, 007 (1998). doi:10.1088/1126-6708/1998/05/007
10. M. Cacciari, S. Frixione, P. Nason, The p_T spectrum in heavy-flavour photoproduction. J. High Energy Phys. **0103**, 006 (2001). doi:10.1088/1126-6708/2001/03/006
11. S. Frixione, P. Nason, B.R. Webber, Matching NLO QCD and parton showers in heavy-flavour production. J. High Energy Phys. **0308**, 007 (2003). doi:10.1088/1126-6708/2003/08/007
12. S. Frixione, B.R. Webber, Matching NLO QCD computations and parton shower simulations. J. High Energy Phys. **0206**, 029 (2002). doi:10.1088/1126-6708/2002/06/029
13. CMS Collaboration, The CMS experiment at the CERN LHC. J. Instrum. **0803**, S08004 (2008). doi:10.1088/1748-0221/3/08/S08004
14. CMS Collaboration, CMS tracking performance results from early LHC operation. Eur. Phys. J. C **70**, 1165 (2010). doi:10.1140/epjc/s10052-010-1491-3
15. T. Sjöstrand, S. Mrenna, P.Z. Skands, PYTHIA 6.4 physics and manual. J. High Energy Phys. **0605**, 026 (2006). doi:10.1088/1126-6708/2006/05/026
16. M. Bargiotti, V. Vagnoni, Heavy quarkonia sector in PYTHIA 6.324: tuning, validation and perspectives at LHC(b). LHCb-2007-042 (2007)
17. D.J. Lange, The EvtGen particle decay simulation package. Nucl. Instrum. Methods A **462**, 152 (2001). doi:10.1016/S0168-9002(01)00089-4
18. E. Barberio, B. van Eijk, Z. Was, PHOTOS—a universal Monte Carlo for QED radiative corrections in decays. Comput. Phys. Commun. **66**, 115 (1991). doi:10.1016/0010-4655(91)90012-A
19. E. Barberio, Z. Was, PHOTOS—a universal Monte Carlo for QED radiative corrections: version 2.0. Comput. Phys. Commun. **79**, 291 (1994). doi:10.1016/0010-4655(94)90074-4
20. S. Agostinelli et al., GEANT4—a simulation toolkit. Nucl. Instrum. Methods A **506**, 250 (2003). doi:10.1016/S0168-9002(03)01368-8
21. CMS Collaboration, Alignment of the CMS silicon tracker during commissioning with cosmic rays. J. Instrum. **5**, T03009 (2010). doi:10.1088/1748-0221/5/03/T03009
22. CMS Collaboration, Precise mapping of the magnetic field in the CMS barrel yoke using cosmic rays. J. Instrum. **5**, T03021 (2010). doi:10.1088/1748-0221/5/03/T03021
23. C. Amsler et al. (Particle Data Group), 2009 Review of Particle Physics and 2009 partial update for the 2010 edition. Phys. Rev. B **667**, 1 (2008)
24. BaBar Collaboration, Study of inclusive production of charmonium mesons in B decays. Phys. Rev. D **67**, 032002 (2003). doi:10.1103/PhysRevD.67.032002
25. M.J. Oreglia, A study of the reactions $\psi' \to \gamma\gamma\psi$. Ph.D. Thesis SLAC-R-236 (1980), Appendix D
26. ALEPH Collaboration, Measurement of the $\bar{B}^0$ and B^- meson lifetimes. Phys. Lett. B **307**, 194 (1993). doi:10.1016/0370-2693(93)90211-Y
27. ALEPH Collaboration, Measurement of the $\bar{B}^0$ and B^- meson lifetimes. Phys. Lett. B **325**, 537 (1994). Erratum
28. H. Jung, The CCFM Monte Carlo generator CASCADE. Comput. Phys. Commun. **143**, 100 (2002). doi:10.1016/S0010-4655(01)00438-6
29. H. Jung et al., The CCFM Monte Carlo generator CASCADE 2.2.0. arXiv:1008.0152

30. A.D. Frawley, T. Ullrich, R. Vogt, Heavy flavor in heavy-ion collisions at RHIC and RHIC II. Phys. Rep. **462**, 125 (2008). doi:10.1016/j.physrep.2008.04.002

31. F. Halzen, CVC for gluons and hadroproduction of quark flavours. Phys. Lett. B **69**, 105 (1977). doi:10.1016/0370-2693(77)90144-7

32. H. Fritzsch, Producing heavy quark flavors in hadronic collisions: a test of Quantum Chromodynamics. Phys. Lett. B **67**, 217 (1977). doi:10.1016/0370-2693(77)90108-3

33. M. Gluck, J.F. Owens, E. Reya, Gluon contribution to hadronic J/ψ production. Phys. Rev. D **17**, 2324 (1978). doi:10.1103/PhysRevD.17.2324

34. V.D. Barger, W.-Y. Keung, R.J.N. Phillips, On ψ and Υ production via gluons. Phys. Lett. B **91**, 253 (1980). doi:10.1016/0370-2693(80)90444-X

35. J. Campbell, F. Maltoni, F. Tramontano, QCD corrections to J/ψ and Υ production at hadron colliders. Phys. Rev. Lett. **98**, 252002 (2007). doi:10.1103/PhysRevLett.98.252002

36. P. Artoisenet et al., Υ production at Fermilab Tevatron and LHC energies. Phys. Rev. Lett. **101**, 152001 (2008). doi:10.1103/PhysRevLett.101.152001

37. P. Artoisenet, J.P. Lansberg, F. Maltoni, Hadroproduction of J/ψ and Υ in association with a heavy-quark pair. Phys. Lett. B **653**, 60 (2007). doi:10.1016/j.physletb.2007.04.031

38. J.P. Lansberg, On the mechanisms of heavy-quarkonium hadroproduction. Eur. Phys. J. C **61**, 693 (2009). doi:10.1140/epjc/s10052-008-0826-9

39. P. Cho, A.K. Leibovich, Colour-octet quarkonia production. Phys. Rev. D **53**, 150 (1996). doi:10.1103/PhysRevD.53.150

40. P. Cho, A.K. Leibovich, Colour-octet quarkonia production II. Phys. Rev. D **53**, 6203 (1996). doi:10.1103/PhysRevD.53.6203

41. Y.-Q. Ma, K. Wang, K.-T. Chao, χ_{cJ} production at hadron colliders with QCD radiative corrections. arXiv:1002.3987

42. P. Faccioli et al., Study of ψ' and χ_c decays as feed-down sources of J/ψ hadro-production. J. High Energy Phys. **10**, 004 (2008). doi:10.1088/1126-6708/2008/10/004

43. Y.-Q. Ma, K. Wang, K.-T. Chao, $J/\psi(\psi')$ production at the Tevatron and LHC at $O(\alpha_s^4 v^4)$ in nonrelativistic QCD. arXiv:1009.3655

44. G.D. Lafferty, T.R. Wyatt, Where to stick your data points: The treatment of measurements within wide bins. Nucl. Instrum. Methods A **355**, 541 (1995). doi:10.1016/0168-9002(94)01112-5

The CMS Collaboration

Yerevan Physics Institute, Yerevan, Armenia
V. Khachatryan, A.M. Sirunyan, A. Tumasyan

Institut für Hochenergiephysik der OeAW, Wien, Austria
W. Adam, T. Bergauer, M. Dragicevic, J. Erö, C. Fabjan, M. Friedl, R. Frühwirth, V.M. Ghete, J. Hammer[1], S. Hänsel, C. Hartl, M. Hoch, N. Hörmann, J. Hrubec, M. Jeitler, G. Kasieczka, W. Kiesenhofer, M. Krammer, D. Liko, I. Mikulec, M. Pernicka, H. Rohringer, R. Schöfbeck, J. Strauss, A. Taurok, F. Teischinger, W. Waltenberger, G. Walzel, E. Widl, C.-E. Wulz

National Centre for Particle and High Energy Physics, Minsk, Belarus
V. Mossolov, N. Shumeiko, J. Suarez Gonzalez

Universiteit Antwerpen, Antwerpen, Belgium
L. Benucci, L. Ceard, E.A. De Wolf, X. Janssen, T. Maes, L. Mucibello, S. Ochesanu, B. Roland, R. Rougny, M. Selvaggi, H. Van Haevermaet, P. Van Mechelen, N. Van Remortel

Vrije Universiteit Brussel, Brussel, Belgium
V. Adler, S. Beauceron, F. Blekman, S. Blyweert, J. D'Hondt, O. Devroede, A. Kalogeropoulos, J. Maes, M. Maes, S. Tavernier, W. Van Doninck, P. Van Mulders, G.P. Van Onsem, I. Villella

Université Libre de Bruxelles, Bruxelles, Belgium
O. Charaf, B. Clerbaux, G. De Lentdecker, V. Dero, A.P.R. Gay, G.H. Hammad, T. Hreus, P.E. Marage, L. Thomas, C. Vander Velde, P. Vanlaer, J. Wickens

Ghent University, Ghent, Belgium
S. Costantini, M. Grunewald, B. Klein, A. Marinov, D. Ryckbosch, F. Thyssen, M. Tytgat, L. Vanelderen, P. Verwilligen, S. Walsh, N. Zaganidis

Université Catholique de Louvain, Louvain-la-Neuve, Belgium
S. Basegmez, G. Bruno, J. Caudron, J. De Favereau De Jeneret, C. Delaere, P. Demin, D. Favart, A. Giammanco, G. Grégoire, J. Hollar, V. Lemaitre, J. Liao, O. Militaru, S. Ovyn, D. Pagano, A. Pin, K. Piotrzkowski, L. Quertenmont, N. Schul

Université de Mons, Mons, Belgium
N. Beliy, T. Caebergs, E. Daubie

Centro Brasileiro de Pesquisas Fisicas, Rio de Janeiro, Brazil
G.A. Alves, D. De Jesus Damiao, M.E. Pol, M.H.G. Souza

Universidade do Estado do Rio de Janeiro, Rio de Janeiro, Brazil
W. Carvalho, E.M. Da Costa, C. De Oliveira Martins, S. Fonseca De Souza, L. Mundim, H. Nogima, V. Oguri, W.L. Prado Da Silva, A. Santoro, S.M. Silva Do Amaral, A. Sznajder, F. Torres Da Silva De Araujo

Instituto de Fisica Teorica, Universidade Estadual Paulista, Sao Paulo, Brazil
F.A. Dias, M.A.F. Dias, T.R. Fernandez Perez Tomei, E.M. Gregores[2], F. Marinho, S.F. Novaes, S.S. Padula

Institute for Nuclear Research and Nuclear Energy, Sofia, Bulgaria
N. Darmenov[1], L. Dimitrov, V. Genchev[1], P. Iaydjiev[1], S. Piperov, M. Rodozov, S. Stoykova, G. Sultanov, V. Tcholakov, R. Trayanov, I. Vankov

University of Sofia, Sofia, Bulgaria
M. Dyulendarova, R. Hadjiiska, V. Kozhuharov, L. Litov, E. Marinova, M. Mateev, B. Pavlov, P. Petkov

Institute of High Energy Physics, Beijing, China
J.G. Bian, G.M. Chen, H.S. Chen, C.H. Jiang, D. Liang, S. Liang, J. Wang, J. Wang, X. Wang, Z. Wang, M. Yang, J. Zang, Z. Zhang

State Key Lab. of Nucl. Phys. and Tech., Peking University, Beijing, China
Y. Ban, S. Guo, W. Li, Y. Mao, S.J. Qian, H. Teng, B. Zhu

Universidad de Los Andes, Bogota, Colombia
A. Cabrera, B. Gomez Moreno, A.A. Ocampo Rios, A.F. Osorio Oliveros, J.C. Sanabria

Technical University of Split, Split, Croatia
N. Godinovic, D. Lelas, K. Lelas, R. Plestina[3], D. Polic, I. Puljak

University of Split, Split, Croatia
Z. Antunovic, M. Dzelalija

Institute Rudjer Boskovic, Zagreb, Croatia
V. Brigljevic, S. Duric, K. Kadija, S. Morovic

University of Cyprus, Nicosia, Cyprus
A. Attikis, R. Fereos, M. Galanti, J. Mousa, C. Nicolaou, F. Ptochos, P.A. Razis, H. Rykaczewski

Academy of Scientific Research and Technology of the Arab Republic of Egypt, Egyptian Network of High Energy Physics, Cairo, Egypt
Y. Assran[4], M.A. Mahmoud[5]

National Institute of Chemical Physics and Biophysics, Tallinn, Estonia
A. Hektor, M. Kadastik, K. Kannike, M. Müntel, M. Raidal, L. Rebane

Department of Physics, University of Helsinki, Helsinki, Finland
V. Azzolini, P. Eerola

Helsinki Institute of Physics, Helsinki, Finland
S. Czellar, J. Härkönen, A. Heikkinen, V. Karimäki, R. Kinnunen, J. Klem, M.J. Kortelainen, T. Lampén, K. Lassila-Perini, S. Lehti, T. Lindén, P. Luukka, T. Mäenpää, E. Tuominen, J. Tuominiemi, E. Tuovinen, D. Ungaro, L. Wendland

Lappeenranta University of Technology, Lappeenranta, Finland
K. Banzuzi, A. Korpela, T. Tuuva

Laboratoire d'Annecy-le-Vieux de Physique des Particules, IN2P3-CNRS, Annecy-le-Vieux, France
D. Sillou

DSM/IRFU, CEA/Saclay, Gif-sur-Yvette, France
M. Besancon, M. Dejardin, D. Denegri, B. Fabbro, J.L. Faure, F. Ferri, S. Ganjour, F.X. Gentit, A. Givernaud, P. Gras, G. Hamel de Monchenault, P. Jarry, E. Locci, J. Malcles, M. Marionneau, L. Millischer, J. Rander, A. Rosowsky, M. Titov, P. Verrecchia

Laboratoire Leprince-Ringuet, Ecole Polytechnique, IN2P3-CNRS, Palaiseau, France

S. Baffioni, F. Beaudette, L. Bianchini, M. Bluj[6], C. Broutin, P. Busson, C. Charlot, L. Dobrzynski, R. Granier de Cassagnac, M. Haguenauer, P. Miné, C. Mironov, C. Ochando, P. Paganini, S. Porteboeuf, D. Sabes, R. Salerno, Y. Sirois, C. Thiebaux, B. Wyslouch[7], A. Zabi

Institut Pluridisciplinaire Hubert Curien, Université de Strasbourg, Université de Haute Alsace Mulhouse, CNRS/IN2P3, Strasbourg, France

J.-L. Agram[8], J. Andrea, A. Besson, D. Bloch, D. Bodin, J.-M. Brom, M. Cardaci, E.C. Chabert, C. Collard, E. Conte[8], F. Drouhin[8], C. Ferro, J.-C. Fontaine[8], D. Gelé, U. Goerlach, S. Greder, P. Juillot, M. Karim[8], A.-C. Le Bihan, Y. Mikami, P. Van Hove

Centre de Calcul de l'Institut National de Physique Nucleaire et de Physique des Particules (IN2P3), Villeurbanne, France

F. Fassi, D. Mercier

Université de Lyon, Université Claude Bernard Lyon 1, CNRS-IN2P3, Institut de Physique Nucléaire de Lyon, Villeurbanne, France

C. Baty, N. Beaupere, M. Bedjidian, O. Bondu, G. Boudoul, D. Boumediene, H. Brun, N. Chanon, R. Chierici, D. Contardo, P. Depasse, H. El Mamouni, A. Falkiewicz, J. Fay, S. Gascon, B. Ille, T. Kurca, T. Le Grand, M. Lethuillier, L. Mirabito, S. Perries, V. Sordini, S. Tosi, Y. Tschudi, P. Verdier, H. Xiao

E. Andronikashvili Institute of Physics, Academy of Science, Tbilisi, Georgia

V. Roinishvili

RWTH Aachen University, I. Physikalisches Institut, Aachen, Germany

G. Anagnostou, M. Edelhoff, L. Feld, N. Heracleous, O. Hindrichs, R. Jussen, K. Klein, J. Merz, N. Mohr, A. Ostapchuk, A. Perieanu, F. Raupach, J. Sammet, S. Schael, D. Sprenger, H. Weber, M. Weber, B. Wittmer

RWTH Aachen University, III. Physikalisches Institut A, Aachen, Germany

M. Ata, W. Bender, M. Erdmann, J. Frangenheim, T. Hebbeker, A. Hinzmann, K. Hoepfner, C. Hof, T. Klimkovich, D. Klingebiel, P. Kreuzer[1], D. Lanske[†], C. Magass, G. Masetti, M. Merschmeyer, A. Meyer, P. Papacz, H. Pieta, H. Reithler, S.A. Schmitz, L. Sonnenschein, J. Steggemann, D. Teyssier

RWTH Aachen University, III. Physikalisches Institut B, Aachen, Germany

M. Bontenackels, M. Davids, M. Duda, G. Flügge, H. Geenen, M. Giffels, W. Haj Ahmad, D. Heydhausen, T. Kress, Y. Kuessel, A. Linn, A. Nowack, L. Perchalla, O. Pooth, J. Rennefeld, P. Sauerland, A. Stahl, M. Thomas, D. Tornier, M.H. Zoeller

Deutsches Elektronen-Synchrotron, Hamburg, Germany

M. Aldaya Martin, W. Behrenhoff, U. Behrens, M. Bergholz[9], K. Borras, A. Cakir, A. Campbell, E. Castro, D. Dammann, G. Eckerlin, D. Eckstein, A. Flossdorf, G. Flucke, A. Geiser, I. Glushkov, J. Hauk, H. Jung, M. Kasemann, I. Katkov, P. Katsas, C. Kleinwort, H. Kluge, A. Knutsson, D. Krücker, E. Kuznetsova, W. Lange, W. Lohmann[9], R. Mankel, M. Marienfeld, I.-A. Melzer-Pellmann, A.B. Meyer, J. Mnich, A. Mussgiller, J. Olzem, A. Parenti, A. Raspereza, A. Raval, R. Schmidt[9], T. Schoerner-Sadenius, N. Sen, M. Stein, J. Tomaszewska, D. Volyanskyy, R. Walsh, C. Wissing

University of Hamburg, Hamburg, Germany

C. Autermann, S. Bobrovskyi, J. Draeger, H. Enderle, U. Gebbert, K. Kaschube, G. Kaussen, R. Klanner, B. Mura, S. Naumann-Emme, F. Nowak, N. Pietsch, C. Sander, H. Schettler, P. Schleper, M. Schröder, T. Schum, J. Schwandt, A.K. Srivastava, H. Stadie, G. Steinbrück, J. Thomsen, R. Wolf

Institut für Experimentelle Kernphysik, Karlsruhe, Germany

J. Bauer, V. Buege, T. Chwalek, D. Daeuwel, W. De Boer, A. Dierlamm, G. Dirkes, M. Feindt, J. Gruschke, C. Hackstein, F. Hartmann, S.M. Heindl, M. Heinrich, H. Held, K.H. Hoffmann, S. Honc, T. Kuhr, D. Martschei, S. Mueller, Th. Müller, M.B. Neuland, M. Niegel, O. Oberst, A. Oehler, J. Ott, T. Peiffer, D. Piparo, G. Quast, K. Rabbertz, F. Ratnikov, M. Renz, A. Sabellek, C. Saout, A. Scheurer, P. Schieferdecker, F.-P. Schilling, G. Schott, H.J. Simonis, F.M. Stober, D. Troendle, J. Wagner-Kuhr, M. Zeise, V. Zhukov[10], E.B. Ziebarth

Institute of Nuclear Physics "Demokritos", Aghia Paraskevi, Greece

G. Daskalakis, T. Geralis, S. Kesisoglou, A. Kyriakis, D. Loukas, I. Manolakos, A. Markou, C. Markou, C. Mavrommatis, E. Petrakou

University of Athens, Athens, Greece
L. Gouskos, T.J. Mertzimekis, A. Panagiotou[1]

University of Ioánnina, Ioánnina, Greece
I. Evangelou, C. Foudas, P. Kokkas, N. Manthos, I. Papadopoulos, V. Patras, F.A. Triantis

KFKI Research Institute for Particle and Nuclear Physics, Budapest, Hungary
A. Aranyi, G. Bencze, L. Boldizsar, G. Debreczeni, C. Hajdu[1], D. Horvath[11], A. Kapusi, K. Krajczar[12], A. Laszlo, F. Sikler, G. Vesztergombi[12]

Institute of Nuclear Research ATOMKI, Debrecen, Hungary
N. Beni, J. Molnar, J. Palinkas, Z. Szillasi, V. Veszpremi

University of Debrecen, Debrecen, Hungary
P. Raics, Z.L. Trocsanyi, B. Ujvari

Panjab University, Chandigarh, India
S. Bansal, S.B. Beri, V. Bhatnagar, N. Dhingra, M. Jindal, M. Kaur, J.M. Kohli, M.Z. Mehta, N. Nishu, L.K. Saini, A. Sharma, A.P. Singh, J.B. Singh, S.P. Singh

University of Delhi, Delhi, India
S. Ahuja, S. Bhattacharya, B.C. Choudhary, P. Gupta, S. Jain, S. Jain, A. Kumar, R.K. Shivpuri

Bhabha Atomic Research Centre, Mumbai, India
R.K. Choudhury, D. Dutta, S. Kailas, S.K. Kataria, A.K. Mohanty[1], L.M. Pant, P. Shukla, P. Suggisetti

Tata Institute of Fundamental Research—EHEP, Mumbai, India
T. Aziz, M. Guchait[13], A. Gurtu, M. Maity[14], D. Majumder, G. Majumder, K. Mazumdar, G.B. Mohanty, A. Saha, K. Sudhakar, N. Wickramage

Tata Institute of Fundamental Research—HECR, Mumbai, India
S. Banerjee, S. Dugad, N.K. Mondal

Institute for Studies in Theoretical Physics & Mathematics (IPM), Tehran, Iran
H. Arfaei, H. Bakhshiansohi, S.M. Etesami, A. Fahim, M. Hashemi, A. Jafari, M. Khakzad, A. Mohammadi, M. Mohammadi Najafabadi, S. Paktinat Mehdiabadi, B. Safarzadeh, M. Zeinali

INFN Sezione di Bari[a], Università di Bari[b], Politecnico di Bari[c], Bari, Italy
M. Abbrescia[a,b], L. Barbone[a,b], C. Calabria[a,b], A. Colaleo[a,b], D. Creanza[a,c], N. De Filippis[a,c], M. De Palma[a,b], A. Dimitrov[a], F. Fedele[a], L. Fiore[a], G. Iaselli[a,c], L. Lusito[a,b,1], G. Maggi[a,c], M. Maggi[a], N. Manna[a,b], B. Marangelli[a,b], S. My[a,c], S. Nuzzo[a,b], N. Pacifico[a,b], G.A. Pierro[a], A. Pompili[a,b], G. Pugliese[a,c], F. Romano[a,c], G. Roselli[a,b], G. Selvaggi[a,b], L. Silvestris[a], R. Trentadue[a], S. Tupputi[a,b], G. Zito[a]

INFN Sezione di Bologna[a], Università di Bologna[b], Bologna, Italy
G. Abbiendi[a], A.C. Benvenuti[a], D. Bonacorsi[a], S. Braibant-Giacomelli[a,b], P. Capiluppi[a,b], A. Castro[a,b], F.R. Cavallo[a], M. Cuffiani[a,b], G.M. Dallavalle[a], F. Fabbri[a], A. Fanfani[a,b], D. Fasanella[a], P. Giacomelli[a], M. Giunta[a], C. Grandi[a], S. Marcellini[a], M. Meneghelli[a,b], A. Montanari[a], F.L. Navarria[a,b], F. Odorici[a], A. Perrotta[a], A.M. Rossi[a,b], T. Rovelli[a,b], G. Siroli[a,b], R. Travaglini[a,b]

INFN Sezione di Catania[a], Università di Catania[b], Catania, Italy
S. Albergo[a,b], G. Cappello[a,b], M. Chiorboli[a,b,1], S. Costa[a,b], A. Tricomi[a,b], C. Tuve[a]

INFN Sezione di Firenze[a], Università di Firenze[b], Firenze, Italy
G. Barbagli[a], V. Ciulli[a,b], C. Civinini[a], R. D'Alessandro[a,b], E. Focardi[a,b], S. Frosali[a,b], E. Gallo[a], C. Genta[a], P. Lenzi[a,b], M. Meschini[a], S. Paoletti[a], G. Sguazzoni[a], A. Tropiano[a,1]

INFN Laboratori Nazionali di Frascati, Frascati, Italy
L. Benussi, S. Bianco, S. Colafranceschi[15], F. Fabbri, D. Piccolo

INFN Sezione di Genova, Genova, Italy
P. Fabbricatore, R. Musenich

INFN Sezione di Milano-Biccoca[a], Università di Milano-Biccoca[b], Milano, Italy

A. Benaglia[a,b], G.B. Cerati[a,b], F. De Guio[a,b,1], L. Di Matteo[a,b], A. Ghezzi[a,b,1], M. Malberti[a,b], S. Malvezzi[a], A. Martelli[a,b], A. Massironi[a,b], D. Menasce[a], L. Moroni[a], M. Paganoni[a,b], D. Pedrini[a], S. Ragazzi[a,b], N. Redaelli[a], S. Sala[a], T. Tabarelli de Fatis[a,b], V. Tancini[a,b]

INFN Sezione di Napoli[a], Università di Napoli "Federico II"[b], Napoli, Italy

S. Buontempo[a], C.A. Carrillo Montoya[a], A. Cimmino[a,b], A. De Cosa[a,b], M. De Gruttola[a,b], F. Fabozzi[a,16], A.O.M. Iorio[a], L. Lista[a], M. Merola[a,b], P. Noli[a,b], P. Paolucci[a]

INFN Sezione di Padova[a], Università di Padova[b], Università di Trento (Trento)[c], Padova, Italy

P. Azzi[a], N. Bacchetta[a], P. Bellan[a,b], D. Bisello[a,b], A. Branca[a], P. Checchia[a], M. De Mattia[a,b], T. Dorigo[a], U. Dosselli[a], F. Fanzago[a], F. Gasparini[a,b], U. Gasparini[a,b], P. Giubilato[a,b], A. Gresele[a,c], S. Lacaprara[a,17], I. Lazzizzera[a,c], M. Margoni[a,b], M. Mazzucato[a], A.T. Meneguzzo[a,b], M. Nespolo[a], L. Perrozzi[a,1], N. Pozzobon[a,b], P. Ronchese[a,b], F. Simonetto[a,b], E. Torassa[a], M. Tosi[a,b], A. Triossi[a], S. Vanini[a,b], P. Zotto[a,b], G. Zumerle[a,b]

INFN Sezione di Pavia[a], Università di Pavia[b], Pavia, Italy

P. Baesso[a,b], U. Berzano[a], C. Riccardi[a,b], P. Torre[a,b], P. Vitulo[a,b], C. Viviani[a,b]

INFN Sezione di Perugia[a], Università di Perugia[b], Perugia, Italy

M. Biasini[a,b], G.M. Bilei[a], B. Caponeri[a,b], L. Fanò[a,b], P. Lariccia[a,b], A. Lucaroni[a,b,1], G. Mantovani[a,b], M. Menichelli[a], A. Nappi[a,b], A. Santocchia[a,b], L. Servoli[a], S. Taroni[a,b], M. Valdata[a,b], R. Volpe[a,b,1]

INFN Sezione di Pisa[a], Università di Pisa[b], Scuola Normale Superiore di Pisa[c], Pisa, Italy

P. Azzurri[a,c], G. Bagliesi[a], J. Bernardini[a,b], T. Boccali[a,1], G. Broccolo[a,c], R. Castaldi[a], R.T. D'Agnolo[a,c], R. Dell'Orso[a], F. Fiori[a,b], L. Foà[a,c], A. Giassi[a], A. Kraan[a], F. Ligabue[a,c], T. Lomtadze[a], L. Martini[a], A. Messineo[a,b], F. Palla[a], F. Palmonari[a], S. Sarkar[a,c], G. Segneri[a], A.T. Serban[a], P. Spagnolo[a], R. Tenchini[a,*], G. Tonelli[a,b,1], A. Venturi[a,1], P.G. Verdini[a]

INFN Sezione di Roma[a], Università di Roma "La Sapienza"[b], Roma, Italy

L. Barone[a,b], F. Cavallari[a], D. Del Re[a,b], E. Di Marco[a,b], M. Diemoz[a], D. Franci[a,b], M. Grassi[a], E. Longo[a,b], G. Organtini[a,b], A. Palma[a,b], F. Pandolfi[a,b,1], R. Paramatti[a], S. Rahatlou[a,b]

INFN Sezione di Torino[a], Università di Torino[b], Università del Piemonte Orientale (Novara)[c], Torino, Italy

N. Amapane[a,b], R. Arcidiacono[a,c], S. Argiro[a,b], M. Arneodo[a,c], C. Biino[a], C. Botta[a,b,1], N. Cartiglia[a], R. Castello[a,b], M. Costa[a,b], N. Demaria[a], A. Graziano[a,b,1], C. Mariotti[a], M. Marone[a,b], S. Maselli[a], E. Migliore[a,b], G. Mila[a,b], V. Monaco[a,b], M. Musich[a,b], M.M. Obertino[a,c], N. Pastrone[a], M. Pelliccioni[a,b,1], A. Romero[a,b], M. Ruspa[a,c], R. Sacchi[a,b], V. Sola[a,b], A. Solano[a,b], A. Staiano[a], D. Trocino[a,b], A. Vilela Pereira[a,b,1]

INFN Sezione di Trieste[a], Università di Trieste[b], Trieste, Italy

F. Ambroglini[a,b], S. Belforte[a], F. Cossutti[a], G. Della Ricca[a,b], B. Gobbo[a], D. Montanino[a,b], A. Penzo[a]

Kangwon National University, Chunchon, Korea

S.G. Heo

Kyungpook National University, Daegu, Korea

S. Chang, J. Chung, D.H. Kim, G.N. Kim, J.E. Kim, D.J. Kong, H. Park, D. Son, D.C. Son

Chonnam National University, Institute for Universe and Elementary Particles, Kwangju, Korea

Zero Kim, J.Y. Kim, S. Song

Korea University, Seoul, Korea

S. Choi, B. Hong, M. Jo, H. Kim, J.H. Kim, T.J. Kim, K.S. Lee, D.H. Moon, S.K. Park, H.B. Rhee, E. Seo, S. Shin, K.S. Sim

University of Seoul, Seoul, Korea

M. Choi, S. Kang, H. Kim, C. Park, I.C. Park, S. Park, G. Ryu

Sungkyunkwan University, Suwon, Korea

Y. Choi, Y.K. Choi, J. Goh, J. Lee, S. Lee, H. Seo, I. Yu

Vilnius University, Vilnius, Lithuania

M.J. Bilinskas, I. Grigelionis, M. Janulis, D. Martisiute, P. Petrov, T. Sabonis

Centro de Investigacion y de Estudios Avanzados del IPN, Mexico City, Mexico

H. Castilla Valdez, E. De La Cruz Burelo, R. Lopez-Fernandez, A. Sánchez Hernández, L.M. Villaseñor-Cendejas

Universidad Iberoamericana, Mexico City, Mexico

S. Carrillo Moreno, F. Vazquez Valencia

Benemerita Universidad Autonoma de Puebla, Puebla, Mexico

H.A. Salazar Ibarguen

Universidad Autónoma de San Luis Potosí, San Luis Potosí, Mexico

E. Casimiro Linares, A. Morelos Pineda, M.A. Reyes-Santos

University of Auckland, Auckland, New Zealand

P. Allfrey, D. Krofcheck, J. Tam

University of Canterbury, Christchurch, New Zealand

P.H. Butler, R. Doesburg, H. Silverwood

National Centre for Physics, Quaid-I-Azam University, Islamabad, Pakistan

M. Ahmad, I. Ahmed, M.I. Asghar, H.R. Hoorani, W.A. Khan, T. Khurshid, S. Qazi

Institute of Experimental Physics, Warsaw, Poland

M. Cwiok, W. Dominik, K. Doroba, A. Kalinowski, M. Konecki, J. Krolikowski

Soltan Institute for Nuclear Studies, Warsaw, Poland

T. Frueboes, R. Gokieli, M. Górski, M. Kazana, K. Nawrocki, M. Szleper, G. Wrochna, P. Zalewski

Laboratório de Instrumentação e Física Experimental de Partículas, Lisboa, Portugal

N. Almeida, A. David, P. Faccioli, P.G. Ferreira Parracho, M. Gallinaro, P. Martins, P. Musella, A. Nayak, P.Q. Ribeiro, J. Seixas, P. Silva, J. Varela[1], H.K. Wöhri

Joint Institute for Nuclear Research, Dubna, Russia

I. Belotelov, P. Bunin, M. Finger, M. Finger Jr., I. Golutvin, A. Kamenev, V. Karjavin, G. Kozlov, A. Lanev, P. Moisenz, V. Palichik, V. Perelygin, S. Shmatov, V. Smirnov, A. Volodko, A. Zarubin

Petersburg Nuclear Physics Institute, Gatchina (St Petersburg), Russia

N. Bondar, V. Golovtsov, Y. Ivanov, V. Kim, P. Levchenko, V. Murzin, V. Oreshkin, I. Smirnov, V. Sulimov, L. Uvarov, S. Vavilov, A. Vorobyev

Institute for Nuclear Research, Moscow, Russia

Yu. Andreev, S. Gninenko, N. Golubev, M. Kirsanov, N. Krasnikov, V. Matveev, A. Pashenkov, A. Toropin, S. Troitsky

Institute for Theoretical and Experimental Physics, Moscow, Russia

V. Epshteyn, V. Gavrilov, V. Kaftanov[†], M. Kossov[1], A. Krokhotin, N. Lychkovskaya, G. Safronov, S. Semenov, I. Shreyber, V. Stolin, E. Vlasov, A. Zhokin

Moscow State University, Moscow, Russia

E. Boos, M. Dubinin[18], L. Dudko, A. Ershov, A. Gribushin, O. Kodolova, I. Lokhtin, S. Obraztsov, S. Petrushanko, L. Sarycheva, V. Savrin, A. Snigirev

P.N. Lebedev Physical Institute, Moscow, Russia

V. Andreev, M. Azarkin, I. Dremin, M. Kirakosyan, S.V. Rusakov, A. Vinogradov

State Research Center of Russian Federation, Institute for High Energy Physics, Protvino, Russia

I. Azhgirey, S. Bitioukov, V. Grishin[1], V. Kachanov, D. Konstantinov, A. Korablev, V. Krychkine, V. Petrov, R. Ryutin, S. Slabospitsky, A. Sobol, L. Tourtchanovitch, S. Troshin, N. Tyurin, A. Uzunian, A. Volkov

University of Belgrade, Faculty of Physics and Vinca Institute of Nuclear Sciences, Belgrade, Serbia

P. Adzic[19], M. Djordjevic, D. Krpic[19], J. Milosevic

Centro de Investigaciones Energéticas Medioambientales y Tecnológicas (CIEMAT), Madrid, Spain

M. Aguilar-Benitez, J. Alcaraz Maestre, P. Arce, C. Battilana, E. Calvo, M. Cepeda, M. Cerrada, N. Colino, B. De La Cruz, C. Diez Pardos, C. Fernandez Bedoya, J.P. Fernández Ramos, A. Ferrando, J. Flix, M.C. Fouz, P. Garcia-Abia, O. Gonzalez Lopez, S. Goy Lopez, J.M. Hernandez, M.I. Josa, G. Merino, J. Puerta Pelayo, I. Redondo, L. Romero, J. Santaolalla, C. Willmott

Universidad Autónoma de Madrid, Madrid, Spain

C. Albajar, G. Codispoti, J.F. de Trocóniz

Universidad de Oviedo, Oviedo, Spain

J. Cuevas, J. Fernandez Menendez, S. Folgueras, I. Gonzalez Caballero, L. Lloret Iglesias, J.M. Vizan Garcia

Instituto de Física de Cantabria (IFCA), CSIC-Universidad de Cantabria, Santander, Spain

J.A. Brochero Cifuentes, I.J. Cabrillo, A. Calderon, M. Chamizo Llatas, S.H. Chuang, J. Duarte Campderros, M. Felcini[20], M. Fernandez, G. Gomez, J. Gonzalez Sanchez, R. Gonzalez Suarez, C. Jorda, P. Lobelle Pardo, A. Lopez Virto, J. Marco, R. Marco, C. Martinez Rivero, F. Matorras, J. Piedra Gomez[21], T. Rodrigo, A. Ruiz Jimeno, L. Scodellaro, M. Sobron Sanudo, I. Vila, R. Vilar Cortabitarte

CERN, European Organization for Nuclear Research, Geneva, Switzerland

D. Abbaneo, E. Auffray, G. Auzinger, P. Baillon, A.H. Ball, D. Barney, A.J. Bell[22], D. Benedetti, C. Bernet[3], W. Bialas, P. Bloch, A. Bocci, S. Bolognesi, H. Breuker, G. Brona, K. Bunkowski, T. Camporesi, E. Cano, G. Cerminara, T. Christiansen, J.A. Coarasa Perez, R. Covarelli, B. Curé, D. D'Enterria, T. Dahms, A. De Roeck, F. Duarte Ramos, A. Elliott-Peisert, W. Funk, A. Gaddi, S. Gennai, G. Georgiou, H. Gerwig, D. Gigi, K. Gill, D. Giordano, F. Glege, R. Gomez-Reino Garrido, M. Gouzevitch, P. Govoni, S. Gowdy, L. Guiducci, M. Hansen, J. Harvey, J. Hegeman, B. Hegner, C. Henderson, H.F. Hoffmann, A. Honma, V. Innocente, P. Janot, E. Karavakis, P. Lecoq, C. Leonidopoulos, C. Lourenço, A. Macpherson, T. Mäki, L. Malgeri, M. Mannelli, L. Masetti, F. Meijers, S. Mersi, E. Meschi, R. Moser, M.U. Mozer, M. Mulders, E. Nesvold[1], M. Nguyen, T. Orimoto, L. Orsini, E. Perez, A. Petrilli, A. Pfeiffer, M. Pierini, M. Pimiä, G. Polese, A. Racz, G. Rolandi[23], T. Rommerskirchen, C. Rovelli[24], M. Rovere, H. Sakulin, C. Schäfer, C. Schwick, I. Segoni, A. Sharma, P. Siegrist, M. Simon, P. Sphicas[25], D. Spiga, M. Spiropulu[18], F. Stöckli, M. Stoye, P. Tropea, A. Tsirou, A. Tsyganov, G.I. Veres[12], P. Vichoudis, M. Voutilainen, W.D. Zeuner

Paul Scherrer Institut, Villigen, Switzerland

W. Bertl, K. Deiters, W. Erdmann, K. Gabathuler, R. Horisberger, Q. Ingram, H.C. Kaestli, S. König, D. Kotlinski, U. Langenegger, F. Meier, D. Renker, T. Rohe, J. Sibille[26], A. Starodumov[27]

Institute for Particle Physics, ETH Zurich, Zurich, Switzerland

P. Bortignon, L. Caminada[28], Z. Chen, S. Cittolin, G. Dissertori, M. Dittmar, J. Eugster, K. Freudenreich, C. Grab, A. Hervé, W. Hintz, P. Lecomte, W. Lustermann, C. Marchica[28], P. Martinez Ruiz del Arbol, P. Meridiani, P. Milenovic[29], F. Moortgat, P. Nef, F. Nessi-Tedaldi, L. Pape, F. Pauss, T. Punz, A. Rizzi, F.J. Ronga, L. Sala, A.K. Sanchez, M.-C. Sawley, B. Stieger, L. Tauscher[†], A. Thea, K. Theofilatos, D. Treille, C. Urscheler, R. Wallny[20], M. Weber, L. Wehrli, J. Weng

Universität Zürich, Zurich, Switzerland

E. Aguiló, C. Amsler, V. Chiochia, S. De Visscher, C. Favaro, M. Ivova Rikova, B. Millan Mejias, C. Regenfus, P. Robmann, A. Schmidt, H. Snoek, L. Wilke

National Central University, Chung-Li, Taiwan

Y.H. Chang, K.H. Chen, W.T. Chen, S. Dutta, A. Go, C.M. Kuo, S.W. Li, W. Lin, M.H. Liu, Z.K. Liu, Y.J. Lu, J.H. Wu, S.S. Yu

National Taiwan University (NTU), Taipei, Taiwan

P. Bartalini, P. Chang, Y.H. Chang, Y.W. Chang, Y. Chao, K.F. Chen, W.-S. Hou, Y. Hsiung, K.Y. Kao, Y.J. Lei, R.-S. Lu, J.G. Shiu, Y.M. Tzeng, M. Wang

Cukurova University, Adana, Turkey

A. Adiguzel, M.N. Bakirci, S. Cerci[30], C. Dozen, I. Dumanoglu, E. Eskut, S. Girgis, G. Gökbulut, Y. Güler, E. Gurpinar, I. Hos, E.E. Kangal, T. Karaman, A. Kayis Topaksu, A. Nart, G. Önengüt, K. Ozdemir, S. Ozturk, A. Polatöz, K. Sogut[31], B. Tali, H. Topakli, D. Uzun, L.N. Vergili, M. Vergili, C. Zorbilmez

Middle East Technical University, Physics Department, Ankara, Turkey

I.V. Akin, T. Aliev, S. Bilmis, M. Deniz, H. Gamsizkan, A.M. Guler, K. Ocalan, A. Ozpineci, M. Serin, R. Sever, U.E. Surat, E. Yildirim, M. Zeyrek

Bogaziçi University, Istanbul, Turkey

M. Deliomeroglu, D. Demir[32], E. Gülmez, A. Halu, B. Isildak, M. Kaya[33], O. Kaya[33], M. Özbek, S. Ozkorucuklu[34], N. Sonmez[35]

National Scientific Center, Kharkov Institute of Physics and Technology, Kharkov, Ukraine

L. Levchuk

University of Bristol, Bristol, United Kingdom

P. Bell, F. Bostock, J.J. Brooke, T.L. Cheng, E. Clement, D. Cussans, R. Frazier, J. Goldstein, M. Grimes, M. Hansen, D. Hartley, G.P. Heath, H.F. Heath, B. Huckvale, J. Jackson, L. Kreczko, S. Metson, D.M. Newbold[36], K. Nirunpong, A. Poll, S. Senkin, V.J. Smith, S. Ward

Rutherford Appleton Laboratory, Didcot, United Kingdom

L. Basso, K.W. Bell, A. Belyaev, C. Brew, R.M. Brown, B. Camanzi, D.J.A. Cockerill, J.A. Coughlan, K. Harder, S. Harper, B.W. Kennedy, E. Olaiya, D. Petyt, B.C. Radburn-Smith, C.H. Shepherd-Themistocleous, I.R. Tomalin, W.J. Womersley, S.D. Worm

Imperial College, London, United Kingdom

R. Bainbridge, G. Ball, J. Ballin, R. Beuselinck, O. Buchmuller, D. Colling, N. Cripps, M. Cutajar, G. Davies, M. Della Negra, J. Fulcher, D. Futyan, A. Guneratne Bryer, G. Hall, Z. Hatherell, J. Hays, G. Iles, G. Karapostoli, L. Lyons, A.-M. Magnan, J. Marrouche, R. Nandi, J. Nash, A. Nikitenko[27], A. Papageorgiou, M. Pesaresi, K. Petridis, M. Pioppi[37], D.M. Raymond, N. Rompotis, A. Rose, M.J. Ryan, C. Seez, P. Sharp, A. Sparrow, A. Tapper, S. Tourneur, M. Vazquez Acosta, T. Virdee, S. Wakefield, D. Wardrope, T. Whyntie

Brunel University, Uxbridge, United Kingdom

M. Barrett, M. Chadwick, J.E. Cole, P.R. Hobson, A. Khan, P. Kyberd, D. Leslie, W. Martin, I.D. Reid, L. Teodorescu

Baylor University, Waco, USA

K. Hatakeyama

Boston University, Boston, USA

T. Bose, E. Carrera Jarrin, A. Clough, C. Fantasia, A. Heister, J. St. John, P. Lawson, D. Lazic, J. Rohlf, D. Sperka, L. Sulak

Brown University, Providence, USA

A. Avetisyan, S. Bhattacharya, J.P. Chou, D. Cutts, S. Esen, A. Ferapontov, U. Heintz, S. Jabeen, G. Kukartsev, G. Landsberg, M. Narain, D. Nguyen, M. Segala, T. Speer, K.V. Tsang

University of California, Davis, Davis, USA

M.A. Borgia, R. Breedon, M. Calderon De La Barca Sanchez, D. Cebra, S. Chauhan, M. Chertok, J. Conway, P.T. Cox, J. Dolen, R. Erbacher, E. Friis, W. Ko, A. Kopecky, R. Lander, H. Liu, S. Maruyama, T. Miceli, M. Nikolic, D. Pellett, J. Robles, T. Schwarz, M. Searle, J. Smith, M. Squires, M. Tripathi, R. Vasquez Sierra, C. Veelken

University of California, Los Angeles, Los Angeles, USA

V. Andreev, K. Arisaka, D. Cline, R. Cousins, A. Deisher, J. Duris, S. Erhan, C. Farrell, J. Hauser, M. Ignatenko, C. Jarvis, C. Plager, G. Rakness, P. Schlein[†], J. Tucker, V. Valuev

University of California, Riverside, Riverside, USA

J. Babb, R. Clare, J. Ellison, J.W. Gary, F. Giordano, G. Hanson, G.Y. Jeng, S.C. Kao, F. Liu, H. Liu, A. Luthra, H. Nguyen, G. Pasztor[38], A. Satpathy, B.C. Shen[†], R. Stringer, J. Sturdy, S. Sumowidagdo, R. Wilken, S. Wimpenny

University of California, San Diego, La Jolla, USA

W. Andrews, J.G. Branson, E. Dusinberre, D. Evans, F. Golf, A. Holzner, R. Kelley, M. Lebourgeois, J. Letts, B. Mangano, J. Muelmenstaedt, S. Padhi, C. Palmer, G. Petrucciani, H. Pi, M. Pieri, R. Ranieri, M. Sani, V. Sharma[1], S. Simon, Y. Tu, A. Vartak, F. Würthwein, A. Yagil

University of California, Santa Barbara, Santa Barbara, USA

D. Barge, R. Bellan, C. Campagnari, M. D'Alfonso, T. Danielson, P. Geffert, J. Incandela, C. Justus, P. Kalavase, S.A. Koay, D. Kovalskyi, V. Krutelyov, S. Lowette, N. Mccoll, V. Pavlunin, F. Rebassoo, J. Ribnik, J. Richman, R. Rossin, D. Stuart, W. To, J.R. Vlimant

California Institute of Technology, Pasadena, USA

A. Apresyan, A. Bornheim, J. Bunn, Y. Chen, M. Gataullin, D. Kcira, V. Litvine, Y. Ma, A. Mott, H.B. Newman, C. Rogan, V. Timciuc, P. Traczyk, J. Veverka, R. Wilkinson, Y. Yang, R.Y. Zhu

Carnegie Mellon University, Pittsburgh, USA

B. Akgun, R. Carroll, T. Ferguson, Y. Iiyama, D.W. Jang, S.Y. Jun, Y.F. Liu, M. Paulini, J. Russ, N. Terentyev, H. Vogel, I. Vorobiev

University of Colorado at Boulder, Boulder, USA

J.P. Cumalat, M.E. Dinardo, B.R. Drell, C.J. Edelmaier, W.T. Ford, B. Heyburn, E. Luiggi Lopez, U. Nauenberg, J.G. Smith, K. Stenson, K.A. Ulmer, S.R. Wagner, S.L. Zang

Cornell University, Ithaca, USA

L. Agostino, J. Alexander, A. Chatterjee, S. Das, N. Eggert, L.J. Fields, L.K. Gibbons, B. Heltsley, W. Hopkins, A. Khukhunaishvili, B. Kreis, V. Kuznetsov, G. Nicolas Kaufman, J.R. Patterson, D. Puigh, D. Riley, A. Ryd, X. Shi, W. Sun, W.D. Teo, J. Thom, J. Thompson, J. Vaughan, Y. Weng, L. Winstrom, P. Wittich

Fairfield University, Fairfield, USA

A. Biselli, G. Cirino, D. Winn

Fermi National Accelerator Laboratory, Batavia, USA

S. Abdullin, M. Albrow, J. Anderson, G. Apollinari, M. Atac, J.A. Bakken, S. Banerjee, L.A.T. Bauerdick, A. Beretvas, J. Berryhill, P.C. Bhat, I. Bloch, F. Borcherding, K. Burkett, J.N. Butler, V. Chetluru, H.W.K. Cheung, F. Chlebana, S. Cihangir, M. Demarteau, D.P. Eartly, V.D. Elvira, I. Fisk, J. Freeman, Y. Gao, E. Gottschalk, D. Green, K. Gunthoti, O. Gutsche, A. Hahn, J. Hanlon, R.M. Harris, J. Hirschauer, B. Hooberman, E. James, H. Jensen, M. Johnson, U. Joshi, R. Khatiwada, B. Kilminster, B. Klima, K. Kousouris, S. Kunori, S. Kwan, P. Limon, R. Lipton, J. Lykken, K. Maeshima, J.M. Marraffino, D. Mason, P. McBride, T. McCauley, T. Miao, K. Mishra, S. Mrenna, Y. Musienko[39], C. Newman-Holmes, V. O'Dell, S. Popescu[40], R. Pordes, O. Prokofyev, N. Saoulidou, E. Sexton-Kennedy, S. Sharma, A. Soha, W.J. Spalding, L. Spiegel, P. Tan, L. Taylor, S. Tkaczyk, L. Uplegger, E.W. Vaandering, R. Vidal, J. Whitmore, W. Wu, F. Yang, F. Yumiceva, J.C. Yun

University of Florida, Gainesville, USA

D. Acosta, P. Avery, D. Bourilkov, M. Chen, G.P. Di Giovanni, D. Dobur, A. Drozdetskiy, R.D. Field, M. Fisher, Y. Fu, I.K. Furic, J. Gartner, S. Goldberg, B. Kim, S. Klimenko, J. Konigsberg, A. Korytov, A. Kropivnitskaya, T. Kypreos, K. Matchev, G. Mitselmakher, L. Muniz, Y. Pakhotin, C. Prescott, R. Remington, M. Schmitt, B. Scurlock, P. Sellers, N. Skhirtladze, D. Wang, J. Yelton, M. Zakaria

Florida International University, Miami, USA

C. Ceron, V. Gaultney, L. Kramer, L.M. Lebolo, S. Linn, P. Markowitz, G. Martinez, J.L. Rodriguez

Florida State University, Tallahassee, USA

T. Adams, A. Askew, D. Bandurin, J. Bochenek, J. Chen, B. Diamond, S.V. Gleyzer, J. Haas, S. Hagopian, V. Hagopian, M. Jenkins, K.F. Johnson, H. Prosper, S. Sekmen, V. Veeraraghavan

Florida Institute of Technology, Melbourne, USA

M.M. Baarmand, B. Dorney, S. Guragain, M. Hohlmann, H. Kalakhety, R. Ralich, I. Vodopiyanov

University of Illinois at Chicago (UIC), Chicago, USA

M.R. Adams, I.M. Anghel, L. Apanasevich, Y. Bai, V.E. Bazterra, R.R. Betts, J. Callner, R. Cavanaugh, C. Dragoiu, E.J. Garcia-Solis, C.E. Gerber, D.J. Hofman, S. Khalatyan, F. Lacroix, C. O'Brien, C. Silvestre, A. Smoron, D. Strom, N. Varelas

The University of Iowa, Iowa City, USA

U. Akgun, E.A. Albayrak, B. Bilki, K. Cankocak[41], W. Clarida, F. Duru, C.K. Lae, E. McCliment, J.-P. Merlo, H. Mermerkaya, A. Mestvirishvili, A. Moeller, J. Nachtman, C.R. Newsom, E. Norbeck, J. Olson, Y. Onel, F. Ozok, S. Sen, J. Wetzel, T. Yetkin, K. Yi

Johns Hopkins University, Baltimore, USA

B.A. Barnett, B. Blumenfeld, A. Bonato, C. Eskew, D. Fehling, G. Giurgiu, A.V. Gritsan, Z.J. Guo, G. Hu, P. Maksimovic, S. Rappoccio, M. Swartz, N.V. Tran, A. Whitbeck

The University of Kansas, Lawrence, USA

P. Baringer, A. Bean, G. Benelli, O. Grachov, M. Murray, D. Noonan, V. Radicci, S. Sanders, J.S. Wood, V. Zhukova

Kansas State University, Manhattan, USA

T. Bolton, I. Chakaberia, A. Ivanov, M. Makouski, Y. Maravin, S. Shrestha, I. Svintradze, Z. Wan

Lawrence Livermore National Laboratory, Livermore, USA

J. Gronberg, D. Lange, D. Wright

University of Maryland, College Park, USA

A. Baden, M. Boutemeur, S.C. Eno, D. Ferencek, J.A. Gomez, N.J. Hadley, R.G. Kellogg, M. Kirn, Y. Lu, A.C. Mignerey, K. Rossato, P. Rumerio, F. Santanastasio, A. Skuja, J. Temple, M.B. Tonjes, S.C. Tonwar, E. Twedt

Massachusetts Institute of Technology, Cambridge, USA

B. Alver, G. Bauer, J. Bendavid, W. Busza, E. Butz, I.A. Cali, M. Chan, V. Dutta, P. Everaerts, G. Gomez Ceballos, M. Goncharov, K.A. Hahn, P. Harris, Y. Kim, M. Klute, Y.-J. Lee, W. Li, C. Loizides, P.D. Luckey, T. Ma, S. Nahn, C. Paus, C. Roland, G. Roland, M. Rudolph, G.S.F. Stephans, K. Sumorok, K. Sung, E.A. Wenger, S. Xie, M. Yang, Y. Yilmaz, A.S. Yoon, M. Zanetti

University of Minnesota, Minneapolis, USA

P. Cole, S.I. Cooper, P. Cushman, B. Dahmes, A. De Benedetti, P.R. Dudero, G. Franzoni, J. Haupt, K. Klapoetke, Y. Kubota, J. Mans, V. Rekovic, R. Rusack, M. Sasseville, A. Singovsky

University of Mississippi, University, USA

L.M. Cremaldi, R. Godang, R. Kroeger, L. Perera, R. Rahmat, D.A. Sanders, D. Summers

University of Nebraska-Lincoln, Lincoln, USA

K. Bloom, S. Bose, J. Butt, D.R. Claes, A. Dominguez, M. Eads, J. Keller, T. Kelly, I. Kravchenko, J. Lazo-Flores, C. Lundstedt, H. Malbouisson, S. Malik, G.R. Snow

State University of New York at Buffalo, Buffalo, USA

U. Baur, A. Godshalk, I. Iashvili, A. Kharchilava, A. Kumar, K. Smith

Northeastern University, Boston, USA

G. Alverson, E. Barberis, D. Baumgartel, O. Boeriu, M. Chasco, K. Kaadze, S. Reucroft, J. Swain, D. Wood, J. Zhang

Northwestern University, Evanston, USA

A. Anastassov, A. Kubik, N. Odell, R.A. Ofierzynski, B. Pollack, A. Pozdnyakov, M. Schmitt, S. Stoynev, M. Velasco, S. Won

University of Notre Dame, Notre Dame, USA

L. Antonelli, D. Berry, M. Hildreth, C. Jessop, D.J. Karmgard, J. Kolb, T. Kolberg, K. Lannon, W. Luo, S. Lynch, N. Marinelli, D.M. Morse, T. Pearson, R. Ruchti, J. Slaunwhite, N. Valls, J. Warchol, M. Wayne, J. Ziegler

The Ohio State University, Columbus, USA

B. Bylsma, L.S. Durkin, J. Gu, C. Hill, P. Killewald, K. Kotov, T.Y. Ling, M. Rodenburg, G. Williams

Princeton University, Princeton, USA

N. Adam, E. Berry, P. Elmer, D. Gerbaudo, V. Halyo, P. Hebda, A. Hunt, J. Jones, E. Laird, D. Lopes Pegna, D. Marlow, T. Medvedeva, M. Mooney, J. Olsen, P. Piroué, X. Quan, H. Saka, D. Stickland, C. Tully, J.S. Werner, A. Zuranski

University of Puerto Rico, Mayaguez, USA

J.G. Acosta, X.T. Huang, A. Lopez, H. Mendez, S. Oliveros, J.E. Ramirez Vargas, A. Zatserklyaniy

Purdue University, West Lafayette, USA

E. Alagoz, V.E. Barnes, G. Bolla, L. Borrello, D. Bortoletto, A. Everett, A.F. Garfinkel, Z. Gecse, L. Gutay, M. Jones, O. Koybasi, A.T. Laasanen, N. Leonardo, C. Liu, V. Maroussov, P. Merkel, D.H. Miller, N. Neumeister, K. Potamianos, I. Shipsey, D. Silvers, A. Svyatkovskiy, H.D. Yoo, J. Zablocki, Y. Zheng

Purdue University Calumet, Hammond, USA

P. Jindal, N. Parashar

Rice University, Houston, USA

C. Boulahouache, V. Cuplov, K.M. Ecklund, F.J.M. Geurts, J.H. Liu, J. Morales, B.P. Padley, R. Redjimi, J. Roberts, J. Zabel

University of Rochester, Rochester, USA

B. Betchart, A. Bodek, Y.S. Chung, P. de Barbaro, R. Demina, Y. Eshaq, H. Flacher, A. Garcia-Bellido, P. Goldenzweig, Y. Gotra, J. Han, A. Harel, D.C. Miner, D. Orbaker, G. Petrillo, D. Vishnevskiy, M. Zielinski

The Rockefeller University, New York, USA

A. Bhatti, L. Demortier, K. Goulianos, G. Lungu, C. Mesropian, M. Yan

Rutgers, the State University of New Jersey, Piscataway, USA

O. Atramentov, A. Barker, D. Duggan, Y. Gershtein, R. Gray, E. Halkiadakis, D. Hidas, D. Hits, A. Lath, S. Panwalkar, R. Patel, A. Richards, K. Rose, S. Schnetzer, S. Somalwar, R. Stone, S. Thomas

University of Tennessee, Knoxville, USA

G. Cerizza, M. Hollingsworth, S. Spanier, Z.C. Yang, A. York

Texas A&M University, College Station, USA

J. Asaadi, R. Eusebi, J. Gilmore, A. Gurrola, T. Kamon, V. Khotilovich, R. Montalvo, C.N. Nguyen, J. Pivarski, A. Safonov, S. Sengupta, A. Tatarinov, D. Toback, M. Weinberger

Texas Tech University, Lubbock, USA

N. Akchurin, C. Bardak, J. Damgov, C. Jeong, K. Kovitanggoon, S.W. Lee, P. Mane, Y. Roh, A. Sill, I. Volobouev, R. Wigmans, E. Yazgan

Vanderbilt University, Nashville, USA

E. Appelt, E. Brownson, D. Engh, C. Florez, W. Gabella, W. Johns, P. Kurt, C. Maguire, A. Melo, P. Sheldon, J. Velkovska

University of Virginia, Charlottesville, USA

M.W. Arenton, M. Balazs, S. Boutle, M. Buehler, S. Conetti, B. Cox, B. Francis, R. Hirosky, A. Ledovskoy, C. Lin, C. Neu, R. Yohay

Wayne State University, Detroit, USA

S. Gollapinni, R. Harr, P.E. Karchin, M. Mattson, C. Milstène, A. Sakharov

University of Wisconsin, Madison, USA

M. Anderson, M. Bachtis, J.N. Bellinger, D. Carlsmith, S. Dasu, J. Efron, L. Gray, K.S. Grogg, M. Grothe, R. Hall-Wilton[1], M. Herndon, P. Klabbers, J. Klukas, A. Lanaro, C. Lazaridis, J. Leonard, D. Lomidze, R. Loveless, A. Mohapatra, W. Parker, D. Reeder, I. Ross, A. Savin, W.H. Smith, J. Swanson, M. Weinberg

†: Deceased

1: Also at CERN, European Organization for Nuclear Research, Geneva, Switzerland

2: Also at Universidade Federal do ABC, Santo Andre, Brazil

3: Also at Laboratoire Leprince-Ringuet, Ecole Polytechnique, IN2P3-CNRS, Palaiseau, France

4: Also at Suez Canal University, Suez, Egypt

5: Also at Fayoum University, El-Fayoum, Egypt

6: Also at Soltan Institute for Nuclear Studies, Warsaw, Poland

7: Also at Massachusetts Institute of Technology, Cambridge, USA

8: Also at Université de Haute-Alsace, Mulhouse, France

9: Also at Brandenburg University of Technology, Cottbus, Germany

10: Also at Moscow State University, Moscow, Russia

11: Also at Institute of Nuclear Research ATOMKI, Debrecen, Hungary

12: Also at Eötvös Loránd University, Budapest, Hungary

13: Also at Tata Institute of Fundamental Research—HECR, Mumbai, India

14: Also at University of Visva-Bharati, Santiniketan, India

15: Also at Facolta' Ingegneria Università di Roma "La Sapienza", Roma, Italy

16: Also at Università della Basilicata, Potenza, Italy

17: Also at Laboratori Nazionali di Legnaro dell'INFN, Legnaro, Italy

18: Also at California Institute of Technology, Pasadena, USA

19: Also at Faculty of Physics of University of Belgrade, Belgrade, Serbia

20: Also at University of California, Los Angeles, Los Angeles, USA

21: Also at University of Florida, Gainesville, USA

22: Also at Université de Genève, Geneva, Switzerland

23: Also at Scuola Normale e Sezione dell' INFN, Pisa, Italy

24: Also at INFN Sezione di Roma; Università di Roma "La Sapienza", Roma, Italy

25: Also at University of Athens, Athens, Greece

26: Also at The University of Kansas, Lawrence, USA

27: Also at Institute for Theoretical and Experimental Physics, Moscow, Russia

28: Also at Paul Scherrer Institut, Villigen, Switzerland

29: Also at University of Belgrade, Faculty of Physics and Vinca Institute of Nuclear Sciences, Belgrade, Serbia

30: Also at Adiyaman University, Adiyaman, Turkey

31: Also at Mersin University, Mersin, Turkey

32: Also at Izmir Institute of Technology, Izmir, Turkey

33: Also at Kafkas University, Kars, Turkey

34: Also at Suleyman Demirel University, Isparta, Turkey

35: Also at Ege University, Izmir, Turkey

36: Also at Rutherford Appleton Laboratory, Didcot, United Kingdom

37: Also at INFN Sezione di Perugia; Università di Perugia, Perugia, Italy

38: Also at KFKI Research Institute for Particle and Nuclear Physics, Budapest, Hungary

39: Also at Institute for Nuclear Research, Moscow, Russia

40: Also at Horia Hulubei National Institute of Physics and Nuclear Engineering (IFIN-HH), Bucharest, Romania

41: Also at Istanbul Technical University, Istanbul, Turkey